भाकृअनुप
ICAR

Research
Bulletin
68

FLOOD INDUCED LAND USE LAND COVER CHANGES AND RIVER DYNAMICS ASSESSMENT IN GUJARAT STATE, INDIA

Atmaram Mishra, C. S. Sharma, S. N. Panda
S. K. Jena, D. K. Panda, A. Kumar

Directorate of Water Management
(Indian Council of Agricultural Research)
Bhubaneswar - 751023, Odisha, INDIA

2014

जल प्रबंधन निदेशालय
D. W. M

D W M

Research Bulletin No. 68

Flood Induced Land Use Land Cover Changes and River Dynamics Assessment in Gujarat State, India

Atmaram Mishra
Senior Researcher, International Water Management Institute,
Southern Africa Office, Pretoria, South Africa

C.S. Sharma
Research Scholar, Department of Agricultural & Food Engineering
IIT, Kharagpur, India

S.N. Panda
Professor, Department of Agricultural & Food Engineering
IIT, Kharagpur, India

S.K. Jena
Principal Scientist, DWM, Bhubaneswar, India

D.K. Panda
Senior Scientist, DWM, Bhubaneswar, India

A. Kumar
Director, DWM, Bhubaneswar, India

Directorate of Water Management
(Indian Council of Agricultural Research)
Bhubaneswar - 751023, Odisha, India

2014

Correct Citation:

Mishra A., Sharma C.S., Panda S.N., Jena S.K., Panda D.K. and Kumar A., 2014. Flood Induced Land Use Land Cover Changes and River Dynamics Assessment in Gujarat State, India. *Bulletin No. 68.* Directorate of Water Management, Indian Council of Agricultural Research, Chandrasekharpur, Bhubaneswar, India, 44p

Published by:

Director,
Directorate of Water management
(Indian Council of Agricultural Research)
Chandrasekharpur, Bhubaneswar-751023 Odisha, India.
Phone: 91-674-2300060 ; EPBAX*:* 91-674-2300010, 2300016
Fax: 91-674-2301651; *Web site:* www.dwm.res.in

Printed at:

S J Technotrade (P) Ltd.
Subarnarekha Chambers,
Plot No : A-9 & 10, Unit – IV,
Bhouma Nagar, Bhubaneswar – 751001
Cell: 9132573795
Email : info.technotrade@gmail.com

PREFACE

Natural climatic hazards like flood, an important hydro-geomorphic process of earth's surface, have different regional and local impacts with significant socio-economic consequences. Flood prone area in India is increasing dramatically. On an average, floods affects an area of approximately 7.5 million hectares (M ha) per year out of 40 M ha flood prone area. The torrential rain that lasted for more than 100 hours in the last week of June 2005 caused severe flood in major rivers of Gujarat State, India.

The present study deals with the changes in land use land cover (LULC), water bodies, drainage network in three worst affected districts (Anand, Vadodara and Kheda) of Gujarat state, India due to severe flood during 2005. The Indian Remote Sensing (IRS) P6 Linear Imaging Self Scanning (LISS) III satellite imageries of pre- and post-flooding periods were used as sources of information. Three classification approaches (unsupervised, supervised, fuzzy based) were used to extract flood induced LULC information and change detection. Pre- and post- flooding periods water bodies information were extracted using radiance image and standard water indices i.e., Normalized Difference Water Index (NDWI) and Modified Normalized Difference Water Index (MNDWI). Geomorphometric analysis of the study area along with drainage network extraction and comparison using two different Digital Elevation Models (DEMs) i.e., Advanced Spaceborne Thermal Emission and Reflection Radiometer (ASTER) and Shuttle Radar Topographic Mission (SRTM) was performed to show the quality and accuracy of both the DEMs. Flood susceptibility regions were identified by depressions mapping. Finally for pre- and post- flooding periods, comparative analysis of magnitude and directional change of drainage networks was done.

Results indicated that soft computing technique such as fuzzy based image classification gave better accuracy and separability amongst classes as compared to hard classification techniques. Results also confirmed the better accuracy of MNDWI in separating water bodies. Geomorphometric analysis indicated that extreme values of elevation and slope affected the moment statistics. The drainage network generated using SRTM DEM was more accurate compared to ASTER. Study confirms that the depressions identified in the study area are more susceptible to flood events. We hope that the study can serve as a reference for future research and be helpful in water resources management, flood management, natural resource management, environmental planning and management, and hazards monitoring and mitigation.

Authors

CONTENTS

1. INTRODUCTION

Managing water resources is a major challenge for the world today. Evolving comprehensive management plan for conservation and utilization of water resources, space technology plays a crucial role. Improved spatial, spectral and temporal resolution data from remote sensing provides unique opportunity towards comprehensive monitoring of water resources dynamics. It can be used effectively in the areas of flood mapping and management, irrigation, assessment of waterlogging, snowmelt-runoff forecasts, reservoir sedimentation, watershed treatment, and drought monitoring.

Flood is one of the major natural disasters that affect many parts of the world. It has been observed that every year there are major floods in both developing and developed countries with different regional and local impacts resulting in common economic and social losses. Besides losing billions of dollars in infrastructure and properties, hundreds (sometimes thousands) of human lives are lost each year due to flood. Destructive floods are common in lower latitude regions, particularly in Asia (Kundzewicz et al., 2009). In India, flood affects vast area of the country, transcending state boundaries. Almost 75% of the annual average rainfall occurs during the monsoon season of four months period (June to September). During monsoon season, about 50% of the annual average rainfall is brought by few intense storms. The intense rainfall is one of the main causes responsible for floods in India. Flood prone area in India is increasing dramatically. Out of 40 million hectares (M ha) of the flood prone area in the country, on an average, floods affect an area of around 7.5 M ha per year (MoWR, 2002). In recent years, flash floods following one day to one-week heavy rainfall have become recurrent event in many countries including India.

Damages due to flood have been increasing each year resulting in economic loss, loss of lives, property and agricultural production as well as affecting activities in the flooded areas. The socio-economic losses and environmental changes such as changes in Land Use and Land Cover (LULC) and drainage pattern following extreme flooding event need to be assessed for future planning and precautionary measures. The analysis of spatial extent and temporal pattern of flood-inundated areas and drainage pattern is of prime importance for mitigation of floods. The non-structural measures for mitigation of flood hazards are very cost effective as compared with structural ones (Jain et al., 2006).

Space technologies play a crucial role in studies related to flood and overall management of water resources. Remote Sensing (RS) and Geographic Information Systems (GIS) are powerful, cost-effective and essential tools for viewing, analyzing, characterizing, assessing the spatio-temporal dynamics (Serra et al., 2008; Sharma et al., 2011), flood forecasting, mapping, monitoring including flood damage assessment, LULC change, extent of damages to crops, river configuration, silt deposits, vulnerable

areas of bank erosion, watershed characteristics, validating numerical inundation models, rainfall run-off analysis (Jain et al., 2005; Dewan et al., 2007; Machado and Ahmad, 2007) and making decisions about land, water and atmospheric components. Improved spatial, spectral, and temporal resolution data from remote sensing are found to be appropriate for flood mapping, monitoring, damage assessment, and forecasting (Patel and Srivastava, 2013). For appropriate flood control, it is necessary to acquire timely and reliable information about the flooded areas, watershed areas, river behaviour and configurations etc. prior to, during and after the flood. Satellite imageries and digital elevation data, thus, form the basic data stock for LULC, flood and water bodies mapping, change detection, flood plain dynamics, river morphology, and geomorphology based studies. Mapping of LULC and water bodies are essential for monitoring and quantifying temporal changes which assist in decision making.

Several established methods/ techniques are available for image classification such as visual interpretation, multi-spectral image classification, band ratioing, contextual multi-temporal classification, object based classification etc. Of these, multi-spectral image classification is most commonly used. Different algorithms and strategies have been developed for feature extraction viz., supervised, unsupervised, and hybrid classification; parametric and nonparametric classifiers; segmentation; artificial neural networks; fuzzy sets; image segmentation and knowledge-based systems etc. Numerous change detection methods such as the pre- and post classification comparisons have been developed to assess variations in LULC (Shalaby and Tateishy, 2007). Of these techniques, post-classification comparison is the most widely used for identifying LULC changes (Singh, 1989; Coppin et al., 2004). Specific remote sensing methods have been developed for delineation of open water bodies which includes Normalized Difference Water Index (NDWI) and Modified Normalized Difference Water Index (MNDWI) (McFeeters, 1996; Xu, 2006; Ji et al., 2009). Mapping of LULC and water bodies of pre- and post- flooding periods provide useful information on spatial distribution of water and the effect of flood. Use of radiance image and water indices for extracting water bodies information for change detection due to extreme flood event has been rarely attempted.

In water resources management, surface topography controls the catchment-scale water transport, spatial distribution of surface water content, and water flow path geometry. Geomorphometric parameters play an important role in hydrological processes and analysis of morphology of river basins. Geomorphometric analysis using GIS methods is very useful in analyzing the surface topography, drainage morphometry (Bhagwat et al., 2011) and various river processes (Bishop and Shroder, 2004). Digital Elevation Model (DEM) is a commonly used approach for mapping river morphology.

DEM have opened up avenues for hydrologic and geomorphologic studies along with investigating natural and anthropogenic influences. It includes, analysis of surface

morphology (Frankel and Dolan, 2007), channel network structure (James et al., 2007), river morphology (Mason et al., 2006; Jones et al., 2007; Notebaert et al., 2009), extraction of hydro-morphometric parameters for flood related study, and the links between terrain and ecological patterns among others. The Shuttle Radar Topographic Mission (SRTM) and Advanced Spaceborne Thermal Emission and Reflection Radiometer (ASTER) topographic products allow detailed analyses of earth surface features and characterize the landscape along with other key variables. In case of DEM comparisons, various methods have been developed to achieve correlation matrices, variogram analysis, fourier and fractal methods, spatial transformation, map algebra, cross tabulation techniques, etc. These methods are commonly applied to raster data and cannot be used for drainage network vector comparison. Vectors and polygons are usually analyzed in a qualitative way, through visual interpretation. In the present study, both raster and vector data are compared.

Slope gradient maps gives information about the areas with the steepest slopes, as these are susceptible to mass movements and higher stream flow/run-off, lowest are susceptible to flooding and can be extracted from elevation map. Elevation maps can be used for evaluation of topographic depressions, which are often linked with water accumulation. Remote sensing and GIS techniques can derive considerably accurate representations of various watershed delineation features (Ozdemir and Bird, 2009). In India, drainage and morphometric characteristics of many river basins have been studied using conventional methods (Reddy et al., 2004).

Drainage networks are one of the major elements in characterizing topography and geometry. Field surveying of drainage networks can give accurate information, but is expensive. Extracting drainage networks from DEM is extremely effective (Martz and Garbrecht, 2007) and time saving method. It is a viable alternative to traditional surveys and manual evaluation of topographic maps. Extracted drainage networks are highly dependent on the accuracy and precision of the DEM used. GIS is a powerful tool for evaluating drainage characteristics, interrelationship between basic drainage parameters and continuous monitoring (Thomas et al., 2012; Henshaw et al., 2013). Dynamics of drainage pattern due to extreme flood events can be studied using temporal images as carried out in the present study. It helps in identifying the measures needed to restore the stability.

Depressions on surface topography play an important role in flood inundation along with water retention and storage. Depressions mapping allow visualizing size and spatial location with geometric properties of depression storages. Researchers carrying out hydrologic modeling using DEMs have noted that depressions are real features in topographically complex landscapes (Mark, 1984; Tribe, 1992). These depressions, although mostly small in size, may have profound impacts on local hydrology.

During last week of June 2005, formation of cyclonic circulation over North Bay of Bengal led to depression and ended with excessive down pour in central and southern part of the country. The torrential rain that lasted for more than 100 hours in the last week of June 2005 caused severe flood in major rivers of Gujarat state, India. Out of 25 districts in the state, flood affected 19 districts (four slightly affected, twelve moderately affected and three severely affected). The worst affected districts were Anand, Vadodara and Kheda. These three districts included about 2000 villages out of 9,000 affected in the State. Due to this flood, crops worth millions of US dollar were destroyed. Around 250,000 people were evacuated, 123 people died, with estimated loss of over 80 billion Indian Rupees (1 US $ = 60 Indian Rupees). Due to the topography and poor drainage network; the villages, cities, roads and other infrastructures were flooded with water. Therefore, it is imperative to apply better scientific approach for the management of extreme hydrological event like flood.

The objective of this present study is to map the flood induced LULC using different classification approaches and identify the changes that have taken place using Indian Remote Sensing P6 Linear Imaging Self Scanning III (IRS P6 LISS III) satellite data for the three worst affected districts. Three classification approaches (unsupervised, supervised and fuzzy rule based technique) were used for mapping LULC for pre- and post-flood period. LULC change between pre- and post-flood periods were evaluated using post classification change matrix method. The changes in water bodies were extracted and analysed using radiance image and standard water indices such as Normalized Difference Water Index (NDWI) and Modified Normalized Difference Water Index (MNDWI). Geomorphometric analysis along with delineation of stream network and their comparison was done using ASTER and SRTM DEMs. An attempt was made to evaluate geomorphometric features using SRTM and ASTER DEMs along with assessing the accuracy and suitability of using the satellite data. The study also explores how DEMs of different sources affect geomorphologic and hydrologic processes. To demonstrate the sensitivities of using different DEMs, two hydrologic applications (ArcHydro and ArcSWAT) were used for delineating drainage networks of the study area. A comparative analysis of reference drainage networks and those extracted from the DEMs along with mapping of depressions for identifying flood susceptible areas was carried out. Finally, comparative analysis of magnitude and directional change of drainage network for pre- and post-flooding periods with reference drainage network was done. This study can serve as a reference for future research and helpful in water resources management, flood management, natural resource management, environmental planning and management and hazards monitoring and mitigation.

2. STUDY AREA AND DATA

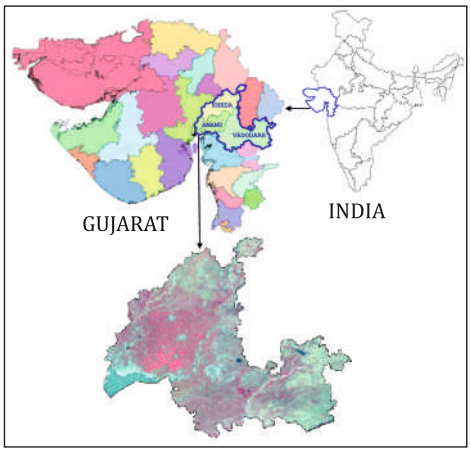

Fig. 1 Location map of the study area

The study area is situated in the Gujarat State, India. The state surrounded by the Arabian Sea in the West, Rajasthan State in the North and North-East, Madhya Pradesh State in the East and Maharashtra State in the South and South East. It lies between 21.1^0 to 24.7^0 N latitude and 68.4^0 to 74.4^0 E longitudes (Fig. 1). The State consists of 25 districts and has a coastline of 1600 km, which forms the western and south western boundaries. On the basis of geographical features, Gujarat is divided into four regions, namely; North Gujarat, South Gujarat, Saurashtra peninsular, and Kachchh. Across the State four different climatic conditions exist, namely, extremely arid, arid, semi-arid and humid. Gujarat mainland covering the central and eastern part of the State receives an average annual rainfall of 800 to 2000 mm, while Saurashtra receives an average annual rainfall of 400 to 800 mm. The average annual rainfall in Kachchh is less than 400 mm. Most of the rain (90-95% of the annual total) falls during the period of June to September, when the southwest monsoon prevails. Water resources in the state are concentrated primarily in the southern and central part of the mainland in which study area falls. The study area comprises of three worst flood affected districts of Gujarat during 2005, Anand (2940.8 km^2), Vadodara (7549.5 km^2), and Kheda (4218.8 km^2). Elevation in the study area ranges from 0-625 m. The mean annual rainfall of the study area is 863 mm and the temperature ranges between 27 and 42^0C. Mahi is the major river along with few medium and minor rivers flowing through the study area. The area is flood prone due to its typical topography and poor drainage characteristics. The study area has experienced number of moderate and severe floods in the past.

2.1 Satellite Imageries and DEM

IRS P6 LISS III satellite imageries were used with resolution of 23.5 m of paths (93-94) and rows (56-57) for LULC classification and mapping water bodies. It provides data in four spectral bands i.e. Green (0.52-0.59 µm), Red (0.62-0.68 µm), Near Infrared (NIR) (0.77-0.86 µm), and Shortwave Infrared (SWIR) (1.55-1.70µm), with 23.5 m spatial resolution and 24 day repeat cycle. The study area is covered in four scenes. In order to capture the hydrological variability of the water bodies due to flood, two time period data i.e. October 2004 (monsoon season) and February 2005 (dry season) were used for pre-flood period. Similarly, October 2005 (monsoon season) and February 2006 (dry season) data were used for post-flood period. In addition, DEMs with two distinct spatial resolutions (30 m ASTER and 90 m SRTM) was used for the extraction of topographic information, drainage network, and depressions in the study area.

3. METHODOLOGY

In the present study, four sets of data (two time periods and two seasons) were used i.e. pre-flood monsoon and dry seasons; Post-flood monsoon and dry seasons (Fig. 2). After radiometric correction, rectification, extraction of study area was done. Normalized Difference Vegetation Index (NDVI) was used for separation of vegetated /non vegetated area. Three classification approaches (unsupervised, supervised, fuzzy based) were used to extract flood induced LULC information followed by accuracy assessment. NDWI and MNDWI indices were used to extract water bodies information. This led to area estimation, analysis and comparison of results obtained from different classification approaches. Post classification change detection was carried out to investigate the changes in LULC and water bodies between pre- and post-flooding periods. Geomorphometric analysis and river network extraction

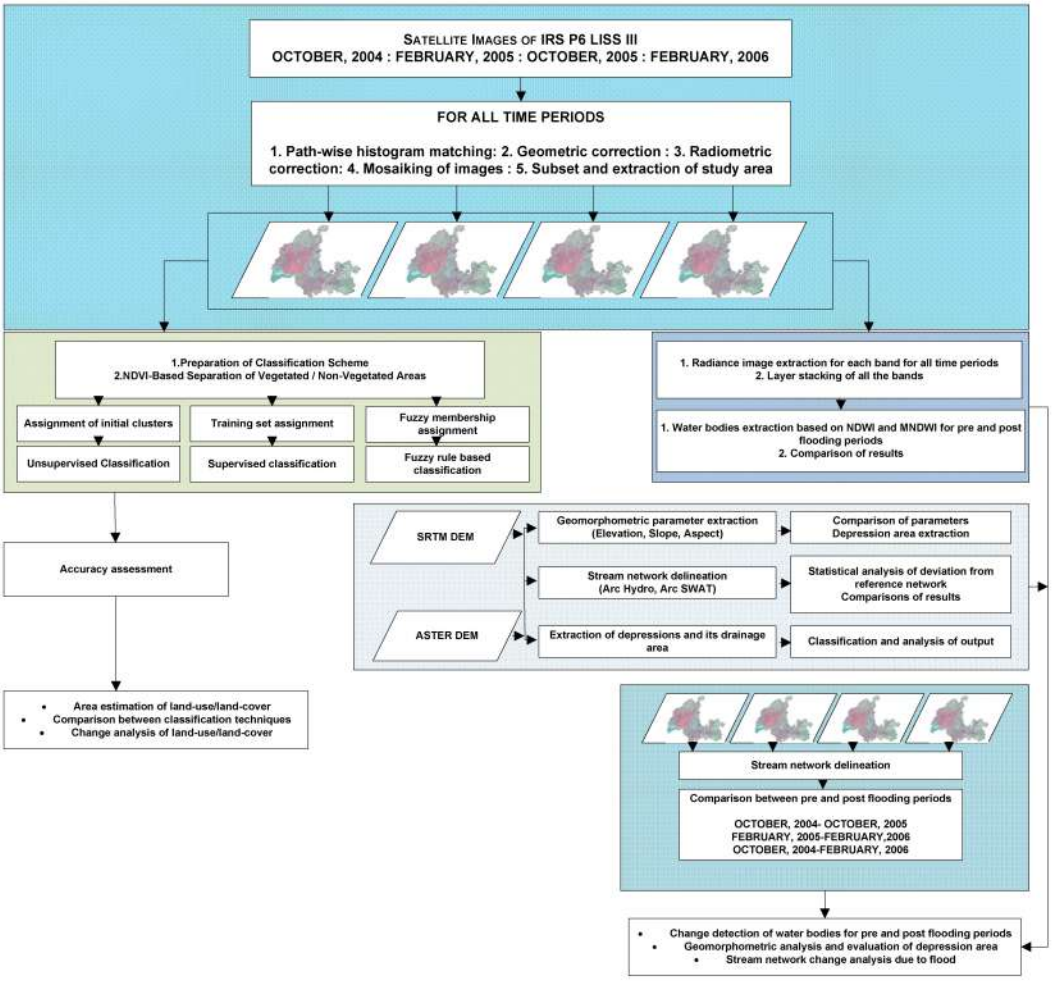

Fig. 2 Overview of methodology

were performed using ASTER and SRTM DEMs. The quality of both the DEMs and geomorphology of the study area was evaluated. Qualitative and quantitative analyses were achieved through visual inspection and examination of slope and aspect obtained from the DEMs, and through the evaluation and comparison of the river networks derived from the available DEMs in ArcHydro and ArcSWAT. Depressions and the drainage area extraction were done to identify the flood susceptibility regions in the study area. Manual delineation of river networks for different time periods was also carried out to study and compare the changes which have taken place primarily due to flood.

3.1 Radiometric and Geometric Corrections

The study area falls under two different paths. Images acquired for extraction of the study area had different radiometric properties for both the paths. Path wise histogram matching was performed to rectify the images. Thereafter, a master scene was geometrically corrected with the base map having Root Mean Square (RMS) error below 0.5. Further, all other scenes were geometrically corrected following image to image registration method with RMS error below 0.6. Due to RMS error value of < 1, geometric correction was acceptable for the present study. RMS error is reported in pixels. It is preferred to tolerate certain amount of error rather than to take a more complex transformation. As in our case, the RMS error tolerance was below 0.6, the retransformed pixel was up to 0.6 pixels away from the source pixel and considered accurate (Leica Geosystems, 2008). Transformation of second order polynomial was performed and resampling was done using nearest neighbor interpolation method with UTM (Universal Transverse Mercator) projection system, spheroid WGS 84 (World Geodetic System) and Zone 43. Subsequently mosaicking was performed and the study area was extracted.

3.2 Classification System for LULC

Classification system provides framework for organizing and categorizing information that can be extracted from image data. A proper classification scheme includes classes that are both important for the study and discernible from the data on hand (Anderson et al., 1976). The level of detailed interpretation from an image primarily depends on the scale. In this case, level 1 classification system was adopted which considers broad classes. Mainly six classes were considered for LULC classification i.e. water bodies (inland), water bodies (coastal), agriculture, agricultural fallow, sparse vegetation (non agricultural and forest), and barren / wasteland. Rivers, streams, reservoir, tanks, and canals were considered under water bodies (inland). As the south-west part of the study area is along the coast, water bodies (coastal) was considered to be an important class. The agricultural and horticultural lands were grouped under the agriculture class. Agricultural fallow consisted of agricultural lands without any vegetation as well

as land just after harvesting. Shrub lands, barren, and sandy area with shrub canopy greater than 60%, shrubs along the river; open forest having canopy between 10 to 40% and some moderate forests were considered under sparse vegetation class. Barren/wasteland class consisted of sandy area along the coast of rivers, dry salt flats, beaches, bare exposed rocks, land without any vegetation, and settlement areas.

3.3 Normalized Difference Vegetation Index (NDVI)

Numerous vegetation indices have been developed to estimate vegetation cover. The most common spectral index used to evaluate vegetation cover is the NDVI (Tucker, 1979). NDVI- based separation of pixels were done to distinguish the vegetative and non-vegetative areas. NDVI uses a set of transformation using Near Infrared (NIR) and Red bands which is as follows:

$$NDVI = \frac{NIR - RED}{NIR + RED} \quad (1)$$

Ideally, values greater than zero represent vegetated area and values less than or equal to zero represent non-vegetated area. Deletion of negative values effectively eliminates the non-vegetation information and retains the vegetation information. During separation it was observed that some other classes are also going with vegetation class, so a threshold point of 0.15 was taken for separation of vegetation and non-vegetation classes. This helped in minimizing the error for getting the training set for classification.

3.4 Classification

In the present study, three classification approaches (unsupervised, supervised, and fuzzy based) were used for mapping of flood induced LULC. Traditional methods of classification are supervised and unsupervised classification that generate one-pixel-to-one-class mapping. Results of traditional classification methods assign crisp boundaries to classes. Crisp class assignment is often inappropriate in geographical and remote sensing sciences. This is because of the uncertainties present in the geographical objects. The study area contains a mixture of land cover classes and these complex combinations of different land cover classes often causes mixed pixels in the remotely sensed data. To quantify uncertainties, it is suggested to use fuzzy approach based on fuzzy sets.

3.4.1 Unsupervised Classification

Unsupervised classification procedure is more automated than supervised classification (Jensen, 2005) and is useful when time is less and high accuracy is not needed. Unsupervised classification algorithms compare pixel spectral signatures to the signatures of computer determined clusters and assign each pixel to one of these clusters (Leica Geosystems, 2008; Lillesand et al., 2008). Unsupervised classification was done using ISO (Iterative Self Organized) Data algorithm. ISO Data algorithm is a

standard unsupervised classifier that uses minimum spectral distance to assign a cluster for each candidate pixel through a number of iterations. In the present study, initially 35 clusters were specified followed by 50 clusters to see whether the ISO Data algorithm has partitioned the feature space effectively. Requesting more clusters and allowing more iteration would partition the feature space even better, so finally 75 clusters were specified. Standard deviation was varied from 0.5 to 3, iteration from 5 to 15 as well as convergence threshold of 0.95 to get desired separability between the classes. These 75 clusters were carefully judged and spectrally similar classes of identical LULC types were merged. The merged clusters were evaluated to see whether they belonged to the desired LULC classes. Finally, a labelling process was carried out to generate a thematic LULC map.

3.4.2 Supervised Classification

In Supervised classification, the spatial patterns in the image dataset are evaluated using predefined decision rules to determine the identity of each pixel. It requires input from an analyst in order to automate the classification algorithm to associate pixel values with the correct land cover category (Jensen, 2005; Lillesand et al., 2008). Supervised classification involves three steps i.e. the training stage, the classification stage, and the output stage. The most common supervised classification techniques are the Maximum Likelihood Classifier (MLC) for parametric input data and Parallelepiped Classifier for non-parametric data.

Initial step for supervised classification was for training site selection and extraction of statistics. We identified homogeneous sample pixels as training pixels (training set data for 6 classes i.e. inland water bodies, coastal water bodies, agriculture, agricultural fallow, sparse vegetation and barren/wasteland) in the image that can be used as representative samples for each LULC category to train the algorithm to locate similar pixels in the image. For each LULC type, fifteen to twenty areas of interest were prepared as the signatures of training samples. The reference data were used to prepare the training signatures. The training areas were created in order to discriminate the individual classes. Only those training data was selected, which gave unimodal histograms per class. Multimodal training data was discarded as it suggests that there are at least two different type of LULC within the training area. After obtaining satisfactory discrimination between the classes during spectral signature evaluation, supervised classification was carried out for all the time period images of the study area.

3.4.3 Image Classification based on Fuzzy Logic

While classifying an image, generally two kinds of problems are faced. First, in most of the cases there is no fixed boundary between two land cover classes. Second, there may be chances of a single pixel containing more than one class. These problems have lead to the concept of soft classification techniques such as sub-pixel classification, fuzzy

classification (Wang, 1990), image segmentation using fuzzy c-mean clustering algorithm etc. In fuzzy classification, fuzzy classifier assigns one pixel to many classes in varying proportions (Foody and Atkinson, 2002). Here, each pixel can belong to several different classes as it does not have definite boundaries (Jensen, 2005).

To handle the concept of "partial truth", Zadeh (1965) proposed a new theory called "Fuzzy Sets". Hard classification procedure may not interpret the boundaries in an appropriate manner, where as the fuzzy approach, in general, deals with the vagueness in the boundaries between classes. Fuzzy set theory provides useful concepts and methods to deal with uncertain information. The set is associated with a membership function and each element in this set has its own membership value towards that particular set. The membership values range between 0 and 1. If the membership value of an element is 0, it means that, it does not belong to that set and if it is 1, then it belongs to that set completely. But, in crisp sets, the membership value is either 1 or 0. A fuzzy classification is used to find out uncertainty in the boundary between classes and to extract the mixed pixel information. This is achieved by applying a function called "membership function" on remotely sensed images. For crisp classification, if a pixel P belongs to a class C, then membership function MF [P, C] = 1, else MF [P, C] = 0. When classes have no definite boundaries, then the assignment of the pixel to a class is uncertain, which is expressed by fuzzy class membership function. It takes the value between 0 and 1, such that CLASS (P) ={C/M [P, C]>0}. In hard classification the assignment implies full membership to single class and no membership to other classes. It is likely that pixel under investigation has different classes also. Such information is completely lost when the pixel is assigned to a single class using hard classification. The sum of membership function values for all classes in each pixel must equal to 1.0. When working with real remote sensor data, the actual fuzzy partition of spectral space is a family of fuzzy sets, F_1, F_2,.....,F_m on the universe X such that for every x which is an element of X (Wang, 1990):

$$0 \leq fF \leq 1 \tag{2}$$

$$\sum_{i}^{n} fF_i(x) > 0 \tag{3}$$

$$\sum_{i}^{m} fF_i(x) = 1 \tag{4}$$

Where F_1, F_2, ..., F_m represents the spectral classes, X represents all pixels in the data sets, m is the number of classes trained upon, n is the number of pixels, x is a pixel measurement vector, and fF is the membership function of the fuzzy sets F_i ($1 \leq i \leq m$). The fuzzy partition may be recorded in a fuzzy partition matrix (Wang, 1990).

$$\begin{pmatrix} fF_1(x_1) & fF_1(x_2) & \ldots\ldots & fF_1(x_n) \\ fF_2(x_1) & fF_2(x_2) & \ldots\ldots & fF_2(x_n) \\ \ldots\ldots & \ldots\ldots & \ldots\ldots & \ldots\ldots \\ fF_m(x_1) & fF_k(x_2) & \ldots\ldots & fF_m(x_n) \end{pmatrix} \quad (5)$$

Where, x_i is the i^{th} pixel's measurement vector ($1 \leq i \leq n$).

Mean and standard deviation values can be taken as parameters for membership function definition and are also used in the present study. The following two equations (Eq. 6 and Eq. 7) describe the fuzzy parameters of the training data:

$$\mu_c^* = \frac{f_c(x_i)x_i}{\sum_{i=1}^{n} f_c(x_i)} \quad (6)$$

$$\sum_c^* = \frac{\sum_{i=1}^{n} f_c(x_i)(x_i - \mu_c^*)(x_i - \mu_c^*)^T}{\sum_{i=1}^{n} f_c(x_i)} \quad (7)$$

Where, the fuzzy mean of training class c is μ_c^*; the fuzzy covariance of training class c is $\sum_c^*$; the vector value of pixel I is x_i; the membership of pixel I x_i to training class c is $f_c(x_i)$; T is the Transpose of the Matrix; n is the total number of pixels of the training data.

In order to determine the fuzzy mean (Eq. 6) and fuzzy covariance (Eq. 7) of every training class, the membership of pixel x_i needs to be known. The membership function is defined based on maximum likelihood classification algorithm with fuzzy mean and fuzzy covariance.

$$f_c(x_i) = \frac{P_c^*(x_i)}{\sum_{j=1}^{m} P_c^*(x_i)} \quad (8)$$

Where, $$P_c^*(x_i) = (2\pi)^{-N/2} \left|\sum_c^*\right|^{-1/2} e^{-1/2\left(x_i - \mu_c^*\right)^T \sum_c^{*-1}\left(x_i - \mu_c^*\right)} \quad (9)$$

Where, the membership of pixel x is $f_c(x_i)$, to class c; the maximum likelihood probability of pixel x_i is $P_c^*(x_i)$, to class c; the number of classes is m and the number of the bands is N.

It is desirable that knowledge automation be incorporated into existing fuzzy systems in order to make the benefits of fuzzy logic available to image classification. Fuzzy based image classification was executed in Matlab and Sugeno method of fuzzy inference system was used. The Sugeno output membership functions are either linear or constant. A typical rule in a Sugeno fuzzy model has the form,

If Input 1 = x and Input 2 = y, then Output $z = ax + by + c$

For a zero-order Sugeno model, the output level z is a constant ($a=b=0$).

3.4.3.1 Membership functions

Membership function is the mathematical function, which defines the degree of an element's membership in a fuzzy set. Univariate statistics such as mean and standard deviation were obtained from training data sets used for supervised classification. It is used as parameters for the fuzzy membership function assignment for fuzzy rule based classification. Input parameters to define membership function for individual LULC class were taken from four individual bands of different time period images. Gaussian Membership functions were defined in each of four bands (Green, Red, NIR, and SWIR) for six LULC classes. Layers of four bands of satellite data were taken as input for classification. After defining membership functions, rules were written for classification.

3.4.3.2 Rules

For six classes, 6 rules were written for fuzzy based classification as given below:

Band1 = = *mf(i)* & Band2= = *mf(i)* & Band3= = *mf(i)* & Band4= = *mf(i)* => Class= = *mf(i)*;

for $(1 \leq i \leq 6)$ (10)

Where, Water bodies (inland) = *mf1*; Water bodies (coastal) = *mf2*; Agriculture = *mf3*; Agricultural fallow = *mf4*; Barren/Wasteland = *mf5*; and Sparse vegetation = *mf6*

Outputs of each rule are combined into a single fuzzy set by aggregation for decision making. Layers of each band were extracted from the images which were used as an input to fuzzy inference system for classification.

3.5 Accuracy Assessment

Accuracy assessment is an essential and most crucial part of studying image classification. The most common and typical method used by researchers to assess classification accuracy is the use of an error matrix (Congalton and Green, 1999; Foody, 2002; Fan et al., 2007). It is also sometimes referred as confusion matrix or contingency table. These tables produce many statistical measures of thematic accuracy including overall classification accuracy, percentage of omission and commission error (Congalton, 1991) and the kappa coefficient, an index that estimates the influence of chance (Yuan et al., 2005).

Accuracy assessment of the classified LULC maps in the present study was based on

reference data, Survey of India topographic maps and visual inspection of high resolution images available on the web (Google Earth). Accuracy assessments of LULC maps were carried out by taking 90 randomly selected points and the results were recorded in an error (confusion) matrix. New points were selected for each LULC map before creating the error matrix to ensure the credibility of accuracy assessment. This was done so that the comparison between error matrices from different classification techniques could be justified. The user's accuracy, producer's accuracy, overall accuracy and the Kappa statistics were obtained in the accuracy assessment report.

3.6 Change Detection

Remote-sensing technologies have provided a tool through which changes can be spatially detected, measured, analyzed, and quantified. Many methods of change detection have been developed to detect LULC change (Mas, 1999). In spite of the numerous evaluations of these techniques, no standard techniques have yet been adopted for all cases. There are many methods of change detection such as image differencing, image ratioing, spectrally based change detection methods such as tasseled cap analysis, vegetation index differencing, change vector analysis, post classification change analysis or thematic change analysis etc. Traditional methods of change detection can be broadly divided in two categories: pre-classification and post-classification methods (Singh, 1989). But post-classification comparison of changes is the most commonly used method for quantitative analysis. In this study, the post-classification change matrix method was used for change detection in LULC, as change matrix gives *to-from* change information about the flood induced LULC for two different time periods.

3.7 Extraction of Water Bodies Information

3.7.1 Conversion to Radiance Image

Atmospheric correction is an important step in the process of land surface reflectance retrieval; therefore, image-based atmospheric correction was carried out initially. On board gain number (LISS-III) for band 2, 3, 4, and 5 are 3, 3, 3, and 2 respectively while the characteristics of IRS P6 are given in Table 1.

Table 1 Characteristics of IRS P6

Band	L_{min}	L_{max}	D_{max}	L_{max}/D_{max}
2	0	12.064	255	0.0473
3	0	15.131	255	0.0593
4	0	15.757	255	0.0618
5	0	3.397	255	0.0133

Remote-sensing satellite detectors show a linear response to incoming radiance. The four time period imageries were radiometrically corrected and calibrated by converting raw digital numbers (DN) into physical units or radiance. The correction was done to minimize the variation due to varying solar-zenith angles and incident solar radiation assuming Lambertian surface. DN values were converted into radiance in a single band using the following formula (Robinove, 1982):

$$L_\lambda = (DN / D_{max}) (L_{max} - L_{min}) + L_{min} \quad (11)$$

Wherein,

L_λ= Radiance in a single band; DN = Digital value of a pixel; D_{max}= Maximum digital number; 255 for bands 1, 2, 3, and 4 of IRS P6; L_{max} = Maximum radiance measured at detector saturation ($mw/cm^2/str/\mu m$); L_{min} = Minimum measured at detector saturation ($mw/cm^2/str/\mu m$)

Equations for calculation of radiance value for different bands are as follows:

Band 2 = $(DN/255)(12.064 - 0) + L_{min}$, Band 3 = $(DN/255)(15.131 - 0) + L_{min}$,

Band 4 = $(DN/255)(15.757 - 0) + L_{min}$, and Band 5 = $(DN/255)(3.397 - 0) + L_{min}$

Radiance images of different bands were layer stacked to get final radiance images for different time periods.

3.7.2 Extraction of Water Bodies

Two-date data pertaining to pre- and post-monsoon of pre- and post-flooding period were used for water bodies mapping. Inland and coastal water bodies (Table 2) were considered for mapping water bodies in the study area. In the present study, multi-band method is used for extraction of water bodies as it takes advantage of reflective differences of each band. The NDWI and MNDWI is a ratio combining two different bands that enhances water spectral signals by contrasting the reflectance between different wavelengths and removing a large portion of noise components in different wavelength regions.

Table 2 Water bodies in the study area

Level I	Level II	Level III
Inland water bodies	Natural	Lakes, Ox-bow Lakes/Cut-off meanders, High altitude Wetlands, Riverine wetlands, Waterlogged area, and River/stream
	Man-made	Reservoirs/ Barrages, Tanks/Ponds, Waterlogged area, and Salt pans
Coastal water bodies	Natural	Lagoons, Creeks, Sand/Beach, Intertidal mud flats, Salt Marsh, Mangroves, and Coral Reefs
	Man-made	Salt pans and Aquaculture ponds

Combinations of the indices/spectral bands used to identify the water body features in the study area are:

i) *Normalised Difference Water Index (NDWI)*

The NDWI is expressed as follows (McFeeters, 1996):

$$\text{NDWI} = \frac{Green - NIR}{Green + NIR} \quad (12)$$

Where, Green is a green band (2) and NIR is a near infrared band (4) of LISS III.

ii) *Modified Normalised Difference Water Index (MNDWI)*

The MNDWI is expressed as (Xu, 2006):

$$\text{MNDWI} = \frac{Green - MIR}{Green + MIR} \quad (13)$$

Where, MIR is a middle infra-red band or SWIR band of LISS III.

3.8 Comparison of DEMs and River Network Extraction

DEM is the most common method for extraction of topographic information. It is often used for delineation of drainage network, catchment boundary, and in estimation of various catchment parameters such as slope, aspects, etc. In the present study, qualitative and quantitative comparison of DEMs at different resolutions is made. The comparison is focused on analyzing how accurately the morphology is represented and affects basin hydrological analysis. ASTER (30 m) and SRTM DEMs (90 m) were used. The ASTER (30 m) was also resampled (90 m) for comparisons. Nearest neighbour method, one of the more popular methods was used for resampling. Methods of resampling do not influence the quality of resampled DEMs significantly. Geomorphometric parameters such as elevation, aspect, and slope angle are useful to identify and describe geomorphological forms and processes. These parameters were extracted and compared. DEMs were processed in ArcGIS 9.3 using ArcHydro and ArcSWAT. Both tools were used for automated drainage network extraction. Minimum threshold area used by ArcHydro for delineation was also used as minimum threshold area for ArcSWAT. In addition, delineation from minimum threshold area provide by ArcSWAT was also performed. After delineation, the extracted streams networks of the study area were compared. The same threshold was applied to both the data sources to facilitate comparison. Extracted drainage networks were compared with reference network (manually delineated drainage network, SOI (Survey of India) topographic maps, and Google Earth), which is assumed to be reasonably accurate. For comparison, 9250 points were randomly selected on base drainage network, which were manually

delineated from satellite image and SOI toposheets. The distances between each drainage point and the nearest point to an extracted vector were calculated.

3.9 Evaluation of Depressions and Drainage Area

Real or natural depressions represent areas of natural storage or man-made modifications to the land surface such as potholes, sinkholes, ponds, detention basins, quarries, lakes and other natural depressions. Surface area and volume of depressions are two parameters that are meaningful since they provide information on the potentially available depression storage in the study area and can help in identification of flood susceptible areas.

Depression in the study area was identified by filling the DEM. It uses the equivalents of several functions such as Focal Flow, Flow Direction, Sink, Watershed, and Zonal Fill to locate and fill sinks. Comparing the original DEM with the filled DEM, the amount, extent and depth of depressions were determined. Parameters obtained from DEM were, number of depressions, number of depression cells, combined surface area of all depressions, combined volume of all depressions, number of cells of each depression, surface area of each depression, and volume of each depression.

3.10 Change Analysis of Extracted Drainage Networks

Due to flood, static and dynamic aspects associated to the drainage network were identified, observed and measured. Drainage network was delineated and extracted for all four time periods (pre- and post-flooding monsoon; Pre- and post-flooding dry season) and compared with a reference drainage network of October, 2004. For comparison, random points were generated on the base drainage network. Distances and angle of orientation from each point on the base drainage network to the extracted vector were determined for each time period.

4. RESULTS AND DISCUSSION

Each classification approach has impact on quantitative spatial extent of LULC as discussed below:

4.1 Unsupervised Classification

Area under different LULC for all the time periods was computed (Table 3 and Figs. 3&4). The estimated area as the percentage of total study area under this classification approach for inland water bodies ranged from 0.86 to 1.37%; coastal water bodies from 2.65 to 2.86%; agriculture from 38.68% to 41.80%; agricultural fallow from 7.42% to 9.68%; sparse vegetation from 28.56% to 29.64%; and barren /wasteland from 17.59 to 17.99% during the period October 2004 to February 2006. It is observed that area occupied by inland water bodies decreased in both the seasons while coastal water bodies increased (6.98%) between October 2004 and October 2005 (Fig. 5) and remained almost same between February 2005 and February 2006. Generally area under inland water bodies is expected to increase in post-flood period. However, results obtained from this classification showed decrease in area. This might be due to misclassification of pixels of inland water bodies. One of the main reasons for misclassification is the similar spectral response of inland water bodies and coastal water bodies. Therefore, careful judgment is necessary before merging and labeling of clusters for each class.

Table 3 Land-use and land-cover in the study area

Sl. No.	Land Use Type	Area (km^2)				Percentage of Total Area (%)			
		October 2004	February 2005	October 2005	February 2006	October 2004	February 2005	October 2005	February 2006
1.	Water Bodies (inland)	[a]205.33	153.98	175.57	129.17	1.37	1.02	1.17	0.86
		[b]121.64	114.42	128.70	106.36	0.81	0.76	0.86	0.71
		[c]141.82	140.61	159.19	130.22	0.94	0.93	1.06	0.87
2.	Water Bodies (coastal)	[a] 398.70	430.42	426.51	429.02	2.65	2.86	2.84	2.85
		[b] 439.95	442.77	446.36	446.00	2.93	2.94	2.97	2.96
		[c] 424.57	425.58	426.54	430.79	2.82	2.83	2.84	2.86
3.	Agriculture	[a]6213.08	6288.76	5814.06	6273.37	41.36	41.80	38.68	41.70
		[b]6225.25	6280.20	5802.99	6260.83	41.42	41.74	38.61	41.62
		[c]6256.50	6292.51	5813.22	6273.40	41.62	41.83	38.74	41.70
4.	Agricultural Fallow	[a]1254.43	1116.04	1455.28	1124.44	8.35	7.42	9.68	7.47
		[b]1287.72	1127.13	1441.07	1112.09	8.57	7.49	9.59	7.39
		[c]1307.09	1139.69	1456.69	1123.63	8.70	7.58	9.71	7.47
5.	Sparse Vegetation	[a]4290.64	4372.32	4454.63	4442.30	28.56	29.06	29.64	29.53
		[b]4272.07	4386.15	4466.16	4460.84	28.42	29.15	29.71	29.65
		[c]4255.5	4372.26	4454.21	4443.61	28.31	29.06	29.68	29.54
6.	Barren/Waste Land	[a]2658.49	2682.87	2704.62	2646.09	17.70	17.83	17.99	17.59
		[b]2684.04	2693.72	2745.39	2658.27	17.86	17.91	18.27	17.67
		[c]2645.19	2673.74	2696.92	2642.74	17.60	17.77	17.97	17.57

Land-use and land-cover obtained from (a) unsupervised classification, (b) supervised classification, and (c) fuzzy classification

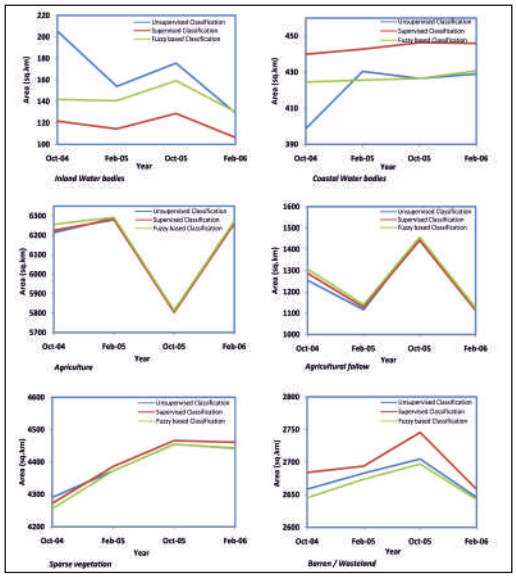

Fig. 3 Area under LULC classes from different classification techniques at different time periods

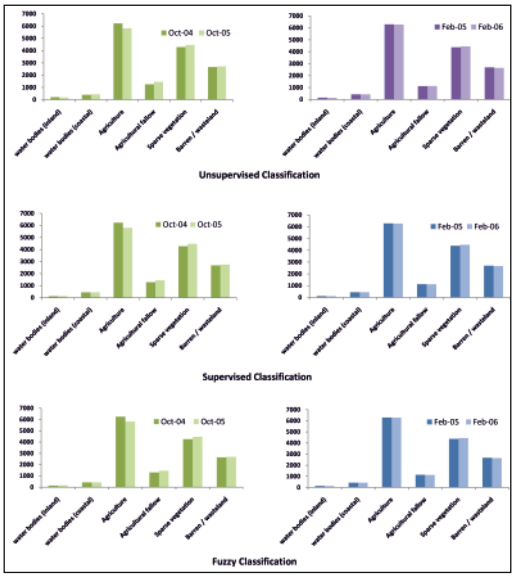

Fig. 4 Area under different LULC in pre- and post-flooding monsoon and dry season using different classification techniques

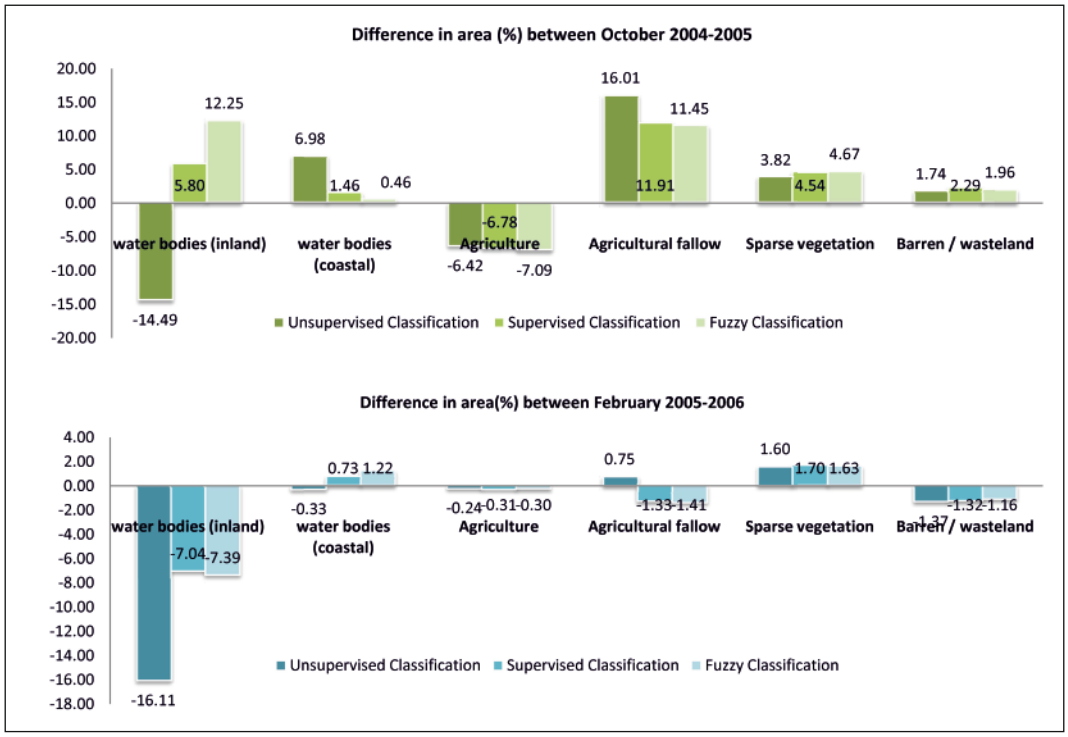

Fig. 5 Comparison of change in area (%) between different seasons

Another significant change was the decline in agricultural area (6.42%) from October 2004 to October 2005, which might be due to the effect of flood occurred just three months before i.e., in June–July 2005. Conversely, agricultural fallow increased (16.01%) between October 2004 and October 2005 and remained approximately same between February 2005 and February 2006, indicating reduction in the effect of flood in the dry season. A small increase in sparse vegetation (3.82%) and barren/wasteland (1.74%) was observed between monsoon of 2004 and 2005. It also indicated an increase of 1.60% for sparse vegetation and decrease of barren/wasteland by 1.37% between winter of 2005 and 2006. Unsupervised classification gave expansive overview of LULC of the study area with some misclassifications. This gave possible scope of further improvement in mapping by using supervised technique.

4.2 Supervised Classification

It was observed that some LULC classes were inaccurately classified in the unsupervised classification as in the case of inland water bodies discussed above. Similarly, some of the sparse vegetation class got merged with agriculture class as it was not possible to separate them due to similar spectral response. Some of the barren / wasteland class was also incorrectly classified as agricultural fallow land. This problem occurred due to spectral in-homogeneity of these classes. For example, a variety of species of bushes, grasses etc. on sparse vegetation, barren / wasteland, and agricultural fallow caused diverse spectral response. Unwanted vegetation (grasses, shrubs etc.) grew in the flood inundated area after flood water receded. Those vegetations on agricultural fallow, sparse vegetation and barren /wastelands gave similar spectral response which led to misclassification between them. Some misclassification in agriculture class also occurred. With supervised classification this ambiguity was taken care and it gave better results as compared to unsupervised classification. The final classified maps of the study area for different time periods are shown in Fig. 6.

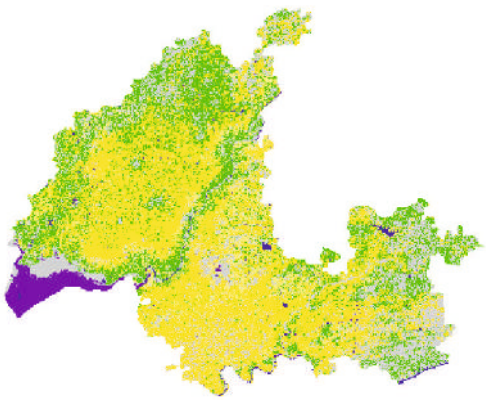

October 2004

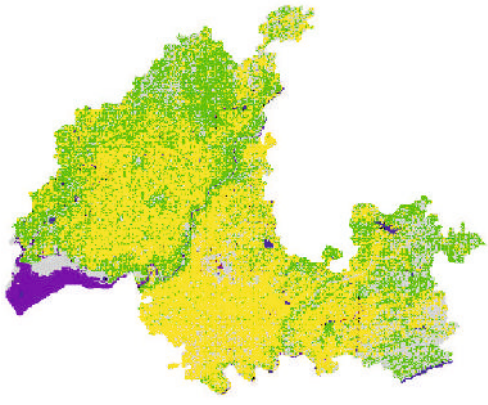

February 2005

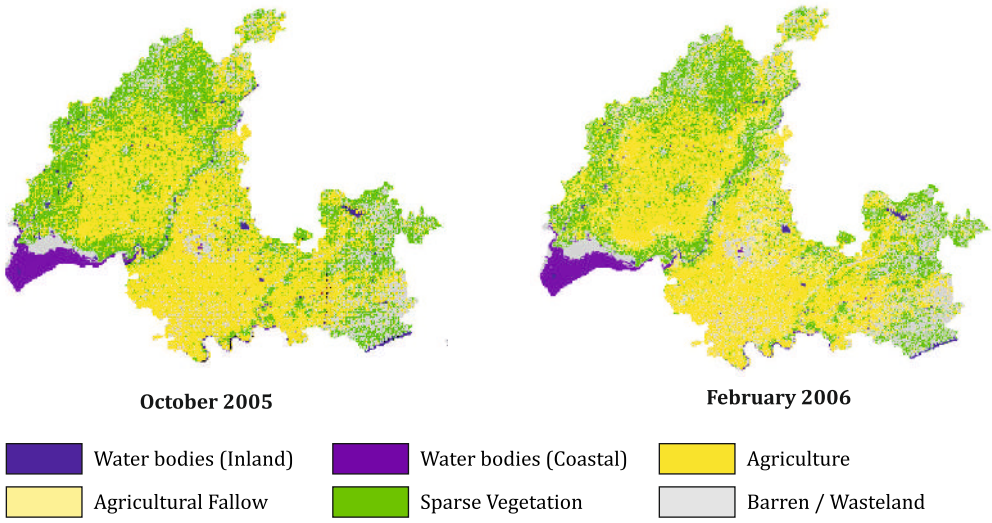

Fig. 6 Land use/Land cover map of the study area for different time periods

The estimated area as the percentage of total area under this classification approach for inland water bodies ranged from 0.71 to 0.86%; coastal water bodies from 2.93 to 2.97%; agriculture from 38.61% to 41.74%; agricultural fallow from 7.39% to 9.59%; sparse vegetation from 28.42% to 29.71%; and barren /wasteland from 17.67 to 18.27% during the period October 2004 to February 2006 (Table 3).

There is an increase in area of inland water bodies (5.80%) during the period October –2004 to October 2005 (Fig. 5). It can be primarily due to the effect of flood, which resulted in increase of water spread area. Conversely, in February 2006 the area under inland water bodies decreased (7.04%) as compared to February 2005. Coastal water bodies area increased in both the time periods. Decrease in agricultural area (6.78%) was observed in October 2005, which is just after the occurrence of flood. In winter approximately same agricultural area was observed indicating decrease in the effect of flood. Agricultural fallow increased by 11.91 % (153.35 km^2) in October 2005. On the contrary, a decrease of 1.33% was noticed in February 2006 as compared to February 2005 indicating that the lands were put under cultivation. Sparse vegetation increased by 4.54% (194.09 km^2) in monsoon season showing the effect of flood but from the increase of 1.70% in winter season indicates that there was gradual reduction in sparse vegetation area from just after flood to February 2006.

The area under inland water bodies decreased (17.66 % - 40.76%) while coastal water bodies (2.87 % - 10.35 %) and barren/wasteland (0.40 % - 1.51 %) increased in all the time periods in case of supervised classification when compared with unsupervised classification. Results from supervised classification showed increased agricultural (0.2%) and decreased sparse vegetation (0.43%) classified area in October 2004 against unsupervised classification. Conversely, for other time periods decrease in agricultural

(0.14% to 0.20%) and increase in sparse vegetation area (0.26% to 0.42%) was observed. In case of agricultural fallow, increase of area in pre-flood seasons and decrease in post-flood season was observed in supervised classification when compared with unsupervised classification. To take account of some fuzziness in classifying the boundary pixels as well as the mixed pixels, fuzzy based classification was done.

4.3 Fuzzy Classification

Individual bands of input parameters that were used to define membership functions (Figs. 7&8) showed an overlap between sparse vegetation and agricultural fallow,

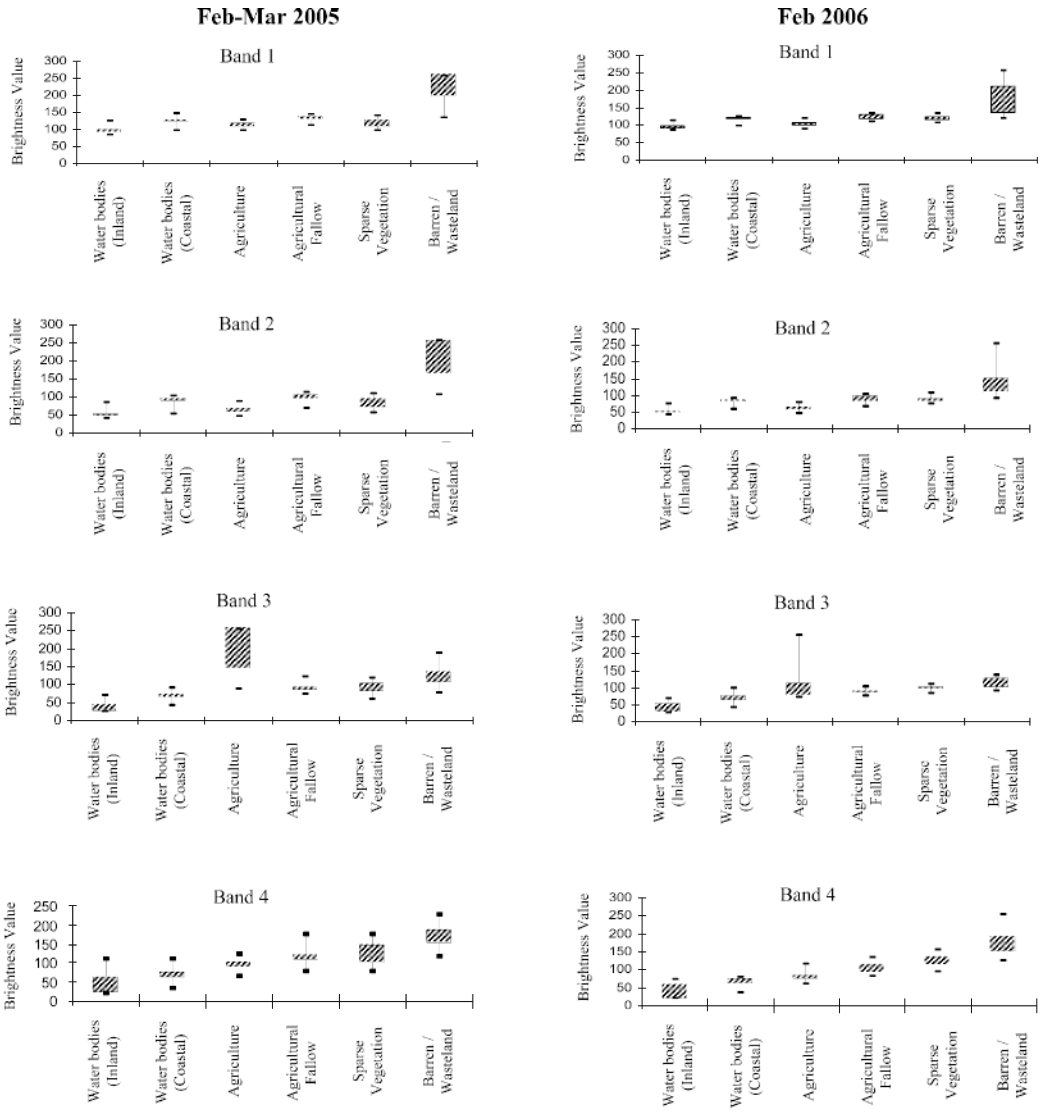

Fig. 7 Class overlaps in different bands for February 2005 and February 2006

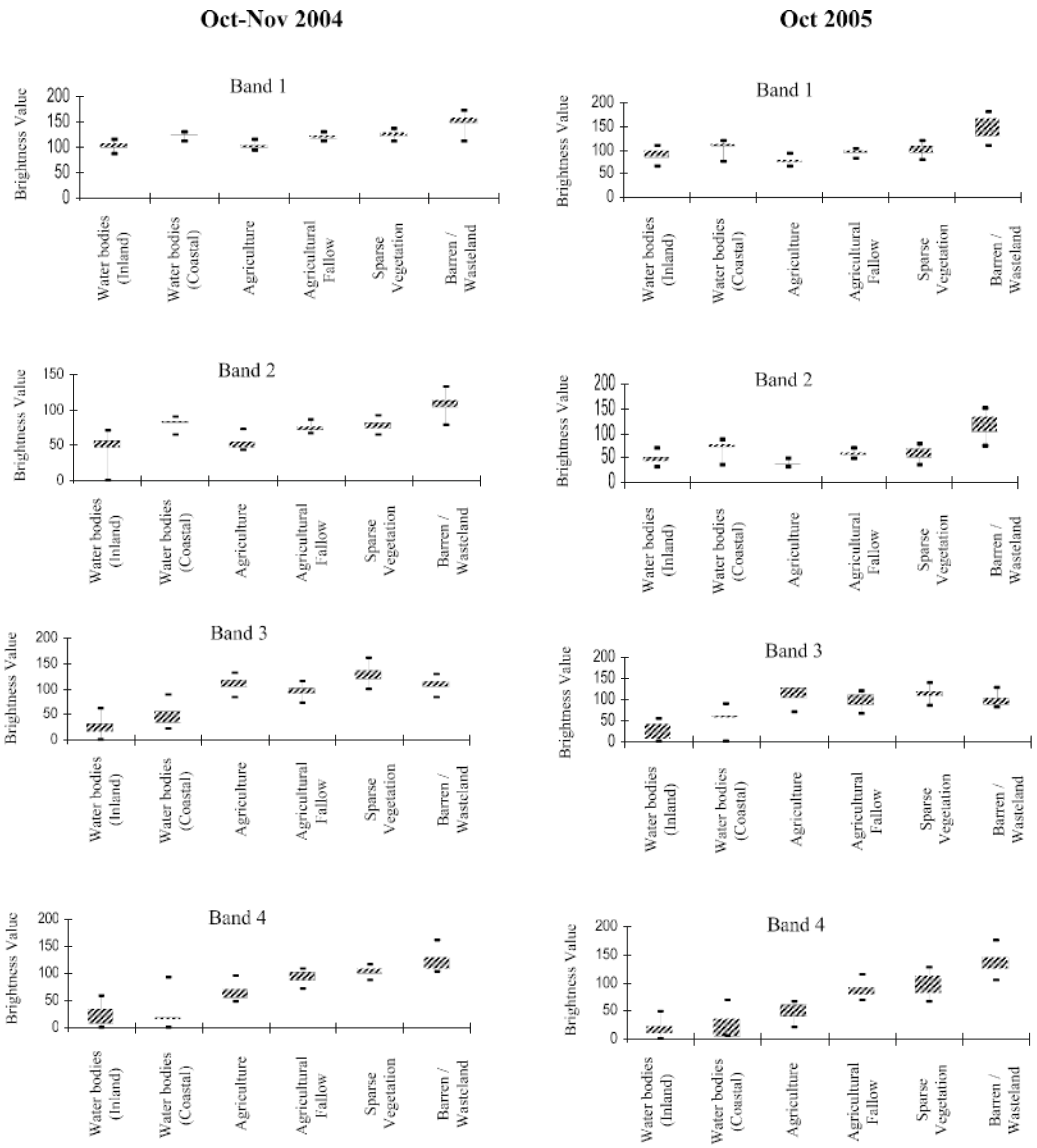

Fig. 8 Class overlaps for different bands in October 2004 and October 2005

which was due to some similar characteristics in spectral response of the classes in the wave length range 0.5-0.59 µm. Since the classification procedure considered multivariate image statistics, this overlap was taken care by other bands for better separability between LULC classes. Agriculture class was well separated specially in NIR band where vegetation cover played an important role with some overlap between agriculture and agricultural fallow. Barren/wasteland with high brightness value was better separated in all the bands except NIR band. Water has high reflectance value in

green band and minimum in NIR band. It was observed that separability of inland and coastal water bodies was acceptable in all the bands.

Fuzzy classification process showed improved separability among LULC classes as compared to supervised classification. Comparison (Fig. 9) showed that in supervised classification, some area of barren land was getting classified under sparse vegetation class, whereas in fuzzy classification the separability was quite satisfactory. Similar trend was seen between inland water bodies and coastal water bodies. Separation among agriculture, agricultural fallow and sparse vegetation was better. The separability among the LULC further increased when the standard deviation was reduced to half of its original value but in most of the cases there was an overlap amongst classes and some unclassified pixels were also generated.

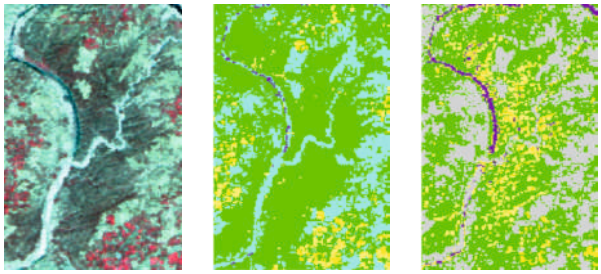

(A) (B) (c)

Fig. 9 A zoomed view of Land use/Land cover classes to compare the results of techniques followed: (A) Original FCC, (B) Supervised classification and (C) Fuzzy classification

Area under different LULC follows similar trend as obtained from supervised classification. In fuzzy based classification, an increase in area (16.59% to 23.69%) for inland water bodies (Fig. 10) was observed in comparison to supervised classification and the increased area have come mostly from coastal water bodies. Agricultural area also increased (0.18% to 0.5%) in different seasons, which came primarily from sparse vegetation. Similar trend was seen for agricultural fallow in which the increased area has come mostly from agriculture.

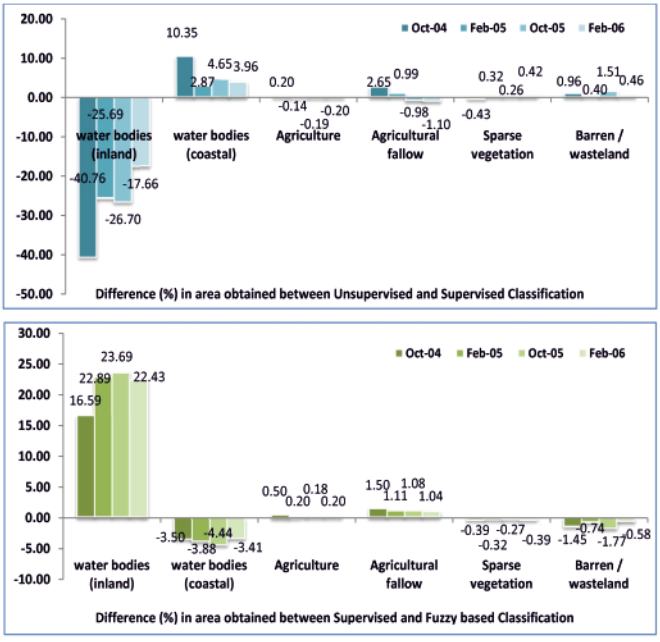

Fig. 10 Comparison of change in area (%) between classification techniques for different LULC classes

The land use area statistics derived from the supervised and fuzzy approaches showed small differences in spatial extent as compared to the unsupervised approach. Automated clustering technique (unsupervised) often failed or overestimated and underestimated, mainly water bodies, agricultural fallow and barren / wastelands. Among the LULC spatial statistics of different classification approaches no high contrast was observed. In this case, the fuzzy approach has shown satisfactory results. However, all classifiers showed little differences in the spatial extent (within ±1% of study area) of the LULC classes.

4.4 Accuracy Assessment

Before using the classification result for change detection, it is important to test the result. Chances of error or misclassification in October 2005 image was most as lots of unwanted vegetation grew on agricultural fallow, sparse vegetation, and barren / wasteland area after the flood water receded. Maximum probability of inaccuracy was possible in classification of image for this time period. So the accuracy assessment of classified LULC map for this time period has been presented. Since the results obtained from accuracy assessment for the other time periods was comparatively similar, they were omitted.

The error matrix correspondent to the final result from different classification process is presented in Tables 4, 5 & 6. In this study, the fuzzy approach appeared to be the best approach. Fuzzy-based classification gave higher overall accuracy and kappa (K^) coefficient than other classification techniques. The overall classification accuracy and kappa statistics (K^) of fuzzy-based classification were 88.82% and 0.87 (Table 4); for supervised classification were 86.76% and 0.84 (Table 5) and for unsupervised classification the respective values were 81.69% and 0.78 (Table 6), respectively. This meets the requirement that K^ values >0.80 (i.e., >80%) representing strong agreement, values between 0.40 and 0.80 (i.e., 40 to 80%) representing moderate agreement and values <0.40 (i.e., <40%) representing poor agreement.

Table 4 Error matrix for fuzzy classification

	Water Bodies (inland)	Water Bodies (coastal)	Agriculture	Agricultural Fallow	Sparse Vegetation	Barren/Waste Land	User's accuracy	Producer's accuracy
Water Bodies (inland)	12	0	0	0	0	0	100.00	92.31
Water Bodies (coastal)	1	14	0	0	0	0	93.33	100.00
Agriculture	0	0	16	1	2	0	84.21	100.00
Agricultural Fallow	0	0	0	11	0	1	91.67	73.33
Sparse Vegetation	0	0	0	1	15	1	88.24	83.33
Barren/Waste Land	0	0	0	2	1	12	80.00	85.71
Overall accuracy = 88.82%, **Kappa statistics** = 0.87								

Table 5 Error matrix for supervised classification

	Water Bodies (inland)	Water Bodies (coastal)	Agriculture	Agricultural Fallow	Sparse Vegetation	Barren/Waste Land	User's accuracy	Producer's accuracy
Water Bodies (inland)	14	2	0	0	0	0	87.50	93.33
Water Bodies (coastal)	1	11	0	0	0	0	91.67	84.62
Agriculture	0	0	16	2	2	0	80.00	88.89
Agricultural Fallow	0	0	0	10	0	1	90.91	76.92
Sparse Vegetation	0	0	2	0	14	0	87.50	82.35
Barren/Waste Land	0	0	0	1	1	13	86.67	92.86
Overall accuracy = 86.76%, **Kappa statistics** = 0.84								

Table 6 Error matrix for unsupervised classification

	Water Bodies (inland)	Water Bodies (coastal)	Agriculture	Agricultural Fallow	Sparse Vegetation	Barren/Waste Land	User's accuracy	Producer's accuracy
Water Bodies (inland)	11	2	0	0	0	0	84.62	78.57
Water Bodies (coastal)	3	12	0	0	0	0	80.00	85.71
Agriculture	0	0	15	2	3	0	75.00	78.95
Agricultural Fallow	0	0	2	11	0	0	84.62	78.57
Sparse Vegetation	0	0	2	0	13	1	81.25	76.47
Barren/Waste Land	0	0	0	1	1	11	84.62	91.67
Overall accuracy = 81.69%, **Kappa statistics** = 0.78								

Fuzzy approach showed an overall accuracy of 88.82% which is close to the overall accuracy (86.76%) of the supervised approach. The fuzzy approach dealt with mixed pixel problems and the heterogeneous representation of LULC. The unsupervised approaches produced lower accuracy (81.69%). Due to the complexity in LULC, the unsupervised approach formed several class clusters in image, creating difficulties in interpretation. However, the unsupervised approach provided better insight to identify certain classes such as agriculture and sparse vegetation in some time periods. The kappa statistics presented a somewhat clearer picture. The kappa coefficient shows that the fuzzy based approach can reduce most of the errors during the classification process. The kappa for the Fuzzy approach was 0.87 (87% reduction of error), which is a bit better than the kappa for the supervised approach of 0.84, with a difference of 2.06% in overall classification accuracy between them. A higher difference of Kappa value (0.06) and accuracy percentage (5.07%) was observed between the supervised and unsupervised approach. This signifies that the supervised approach performed better than the unsupervised in mapping the flood induced LULC.

The overall accuracy and kappa coefficient value only represent the average result. It is still difficult to determine which approach showed refined mapping of LULC at the class level. Fuzzy and supervised approaches exhibited high (>80%) producer's accuracies or low omission errors in all classes except agricultural fallow. User's accuracy for fuzzy and supervised classification also exhibited high value (>80%) for all LULC classes. Mapping of LULC improved to a great extent by the fuzzy approach, showing over 84% user's accuracies. The fuzzy approach, with an user's accuracy of 100%, appeared to be better than the supervised approach (user's accuracy of 87.50%), an increase of 12.50% for extracting inland water bodies. The user's accuracies show that the supervised approach estimates the barren / wasteland class better than the other approaches. In the supervised approach, despite a producer's accuracy of 93.33% for the inland water bodies, there was actually 87.50% user's accuracy, which means at least 5.83% of the inland water bodies were classified erroneously.

The results obtained from the accuracy assessment above indicate that classified LULC maps have sufficient accuracy for post classification comparison approach of change detection. Perusal of the error matrix reveals that there is diminutive confusion in discriminating agriculture from agricultural fallow and sparse vegetation; and barren / wasteland from agricultural fallow and sparse vegetation. Similar diminutive confusion also existed among agricultural fallow and barren / wasteland, sparse vegetation and agriculture. Keeping in view the heterogeneity of different classes present in the study area, the classification accuracies obtained is in fair agreement. Although the classified result has some misinterpreted classes but overall it shows good result in terms of overall accuracy, user's accuracy, producer's accuracy and kappa coefficient to perform change detection.

4.5 Change Detection

Change detection analysis was carried out for pre- and post-flood data of same season, i.e., between October 2004 and October 2005 (monsoon season); and between February 2005 and February 2006 (dry season). Change maps for both the seasons are shown in Figs. 11 and 12. Out of three districts, Anand was the most affected one due to

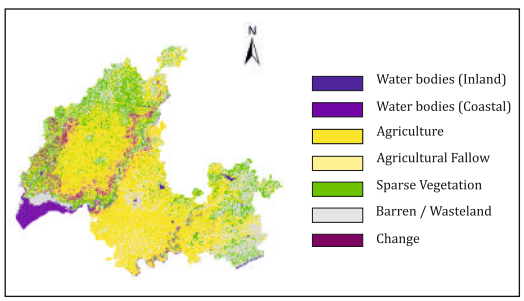

Fig. 11 Land-use/land-cover map for October 2004-October 2005

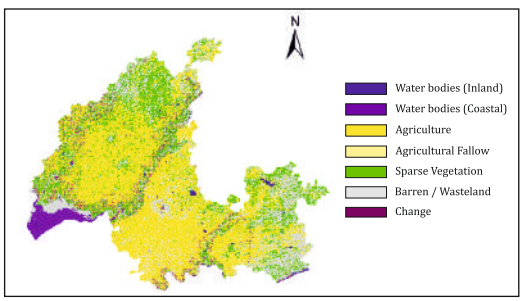

Fig. 12 Land-use/land-cover map for February 2005-February 2006

its topography and location. Flood plains along the river were mostly affected and exhibited major changes. The change matrix analysis was carried out using supervised classification results. The LULC change matrix of the study area for the monsoon and dry season is shown in Tables 7 and 8, respectively.

Table 7 Change detection for October-November 2004 and October 2005

Class		October–November 2004 (Area km²)					
		Water Bodies (Inland)	Water Bodies (coastal)	Agriculture	Agricultural Fallow	Sparse Vegetation	Barren/ Waste land
October 2005 (Area km²)	Water Bodies (Inland)	116.63	7.09	2.89	1.20	0.38	0.51
	Water Bodies (coastal)	2.47	431.28	0.57	5.04	3.60	3.40
	Agriculture	0.30	0.13	5627.38	47.95	119.43	7.80
	Agricultural Fallow	0.49	0.52	212.43	1030.19	164.80	32.64
	Sparse Vegetation	0.71	0.30	306.80	103.45	3912.21	142.69
	Barren/Wasteland	1.04	0.63	75.19	99.89	71.65	2496.99

Table 8 Change detection for February -March 2005 and February 2006

Class		February-March 2005 (Area km²)					
		Water Bodies (Inland)	Water Bodies (coastal)	Agriculture	Agricultural Fallow	Sparse Vegetation	Barren/ Waste land
February 2006 (Area km²)	Water Bodies (Inland)	95.24	0.91	8.19	0.18	1.17	0.67
	Water Bodies (coastal)	9.82	429.7	1.04	1.25	2.24	1.95
	Agriculture	5.79	3.42	5964.8	73.44	200.62	12.76
	Agricultural Fallow	1.47	4.32	80.37	934.04	83.33	8.56
	Sparse Vegetation	0.23	3.01	214.57	111.81	3993.3	137.92
	Barren/Wasteland	1.87	1.41	11.23	6.41	105.49	2531.86

From the change matrix (Tables 7 and 8), changes to-from were analyzed. There was an increase in inland water bodies in October 2005, i.e. 7.09 km^2 of coastal water bodies area got converted to inland water bodies (Table 7). Agricultural area decreased in October 2005, i.e. 212.43 km^2 went to agricultural fallow and 306.80 km^2 to sparse vegetation. Increase of area under sparse vegetation was also observed with area appeared to coming from agricultural land (306.80 km^2), agricultural fallow (103.45 km^2) and barren / wasteland (142.69 km^2). Decrease in area under inland water bodies and minimal increase in coastal water bodies (Table 8) was observed between February 2005 and February 2006. Agriculture and agricultural fallow land decreased but the decrease was not significant. 80.37 km^2 areas became agricultural fallow and on the other hand 73.44 km^2 area of agricultural fallow land was used for cultivation. Area covered under sparse vegetation increased which came from agriculture (214.57

km^2), agricultural fallow (111.81 km^2) and barren wasteland (137.92 km^2). There has been interchange of areas between agriculture, agricultural fallow, sparse vegetation and barren / wasteland in both the time periods. It can be inferred from above discussion that between February 2005 and February 2006, LULC changes due flood in the study area was relatively stable as compared to October 2004 and October 2005. Results obtained from change detection can be considered satisfactory as evident from the accuracy assessments of LULC map.

In supervised classification, simple difference in area of individual LULC classes observed in both the time periods with respect to the total study area showed (Table 1) decrease of around 2% in agriculture and increase of approximately 2% in sparse vegetation between October 2004 and 2005. Similarly, decrease of around 1% in agriculture and increase of approximately 1% in sparse vegetation area was observed between February 2005 and 2006. But in fuzzy based classification (Table 1), decrease of around 3% in agriculture and increase of approximately 1% in agricultural fallow, sparse vegetation, and barren / wasteland area was observed between October 2004 and 2005. Minimal changes in LULC were observed between February 2005 and 2006. Area of individual LULC classes observed in both the time periods for different classification techniques is shown in Fig. 4.

4.6 Extraction of Water Bodies

Application of the NDWI in water regions with a built-up land background does not give satisfactory result as expected. Many built-up land features in the study area have positive values in the NDWI image indicating that the extracted water information in those regions was often mixed with built-up land. The spectral reflectance pattern of built-up land in the green and NIR bands is similar with that of water and often mixed with built-up land. Analysis showed that the average digital number of middle infrared (MIR) radiation is much greater than that of green band. Therefore, if a MIR band is used instead of the NIR band in the NDWI, water feature will have increased value and the built-up land should have negative values. Based on this assumption, the MNDWI was used. Compared with the NDWI, the contrast between water and built-up land of the MNDWI was enhanced resulting in increased values of water feature and decreased values of built-up land from positive down to negative. The greater enhancement of water in the MNDWI image resulted in more accurate extraction of open water features as the built-up land, soil and vegetation (all negative values) is notably suppressed and even removed. In the present study, NDWI exhibited limitations in detecting water features, corroborating its inadequacy for precise water delineation. The MNDWI had better performances in separating water bodies, confirming the better accuracy of indices that incorporate the MIR band.

Area under water bodies was found to be 748 km^2 (October, 2004) and 696 km^2

(February, 2005) for pre-flood period. Similarly, during post-flood period the areas were 826 km^2 (October, 2005) and 723 km^2 (February, 2006). Major increase of water surface area in October, 2005 as compared to October, 2004 indicates the effect of flood in inundating the study area (Fig. 13). In February, 2006 the effect of flood decreased as indicated by the area of water bodies. Difference between the reduced areas during February, 2005-06 as compared to October, 2004-05 indicated restoration of situation to normalcy in February 2006. Mapping of water bodies of both the seasons for pre- and post-flooding periods provided useful information regarding spatial water distribution in the study area. It can help in flood related study where the assessment of water resources is of prime importance.

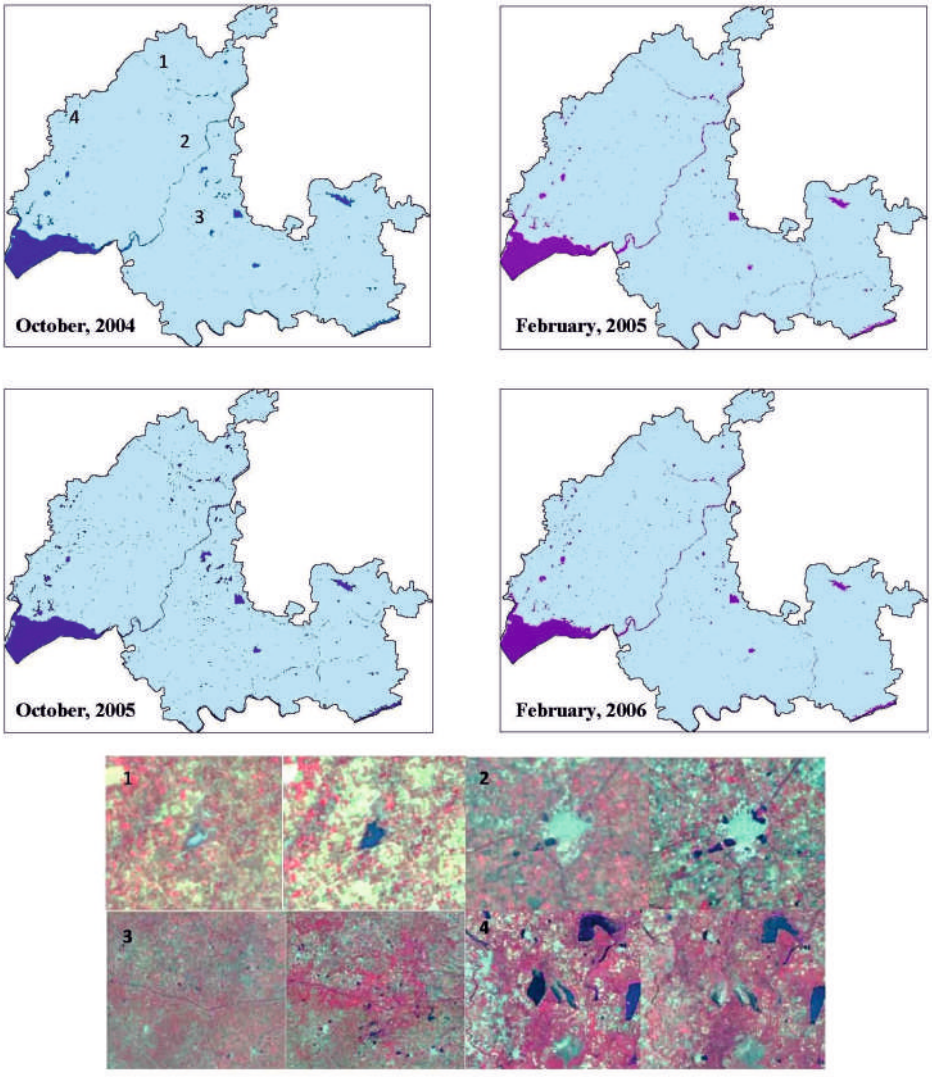

Fig. 13 Water bodies in different time period and changes due to flood (October, 2004-2005)

4.7 Geomorphometric Analysis of DEMs

Elevation information of the study area varies for both ASTER (-6 - 613 m) and SRTM DEM (0 - 625 m). This indicates some difference in elevation information and uncertainty in DEM. It is expected that different sources of DEM will provide slightly different results. The study area is relatively flat in topography with major portion falling below 100 m elevation. When flood occurs in such area, magnitude of impact becomes more sensitive to the level of rising water, and thus an accurate terrain map is crucial in determining the magnitude of flood impacts.

It has been observed that the extreme values of elevation and slope affected the moment statistics of both the DEMs (Fig. 14). Slope was calculated using 8 neighbors (even) method. ASTER and SRTM DEM showed maximum slope of 109.04% (47.5°) and 90.40% (42.1°); average slope of 3.86% (2.2°) and 2.13% (1.2°); standard deviation of 4.85 (%) and 4.29 (%); and RMS of 6.20% and 4.79%, respectively. Study area is relatively flat up to an elevation of 100 m, there is a gradual increase in slope for elevation from 200-300 m, and above 300 m there is variability in slope with elevation. Fig. 15 shows comparison of both the DEMs, including histogram of elevation, percentage of region, concentration, average slope, cumulative percentage area, graph showing concentration by slope, normalized elevation distribution (Strahler, 1952), and scatter plot.

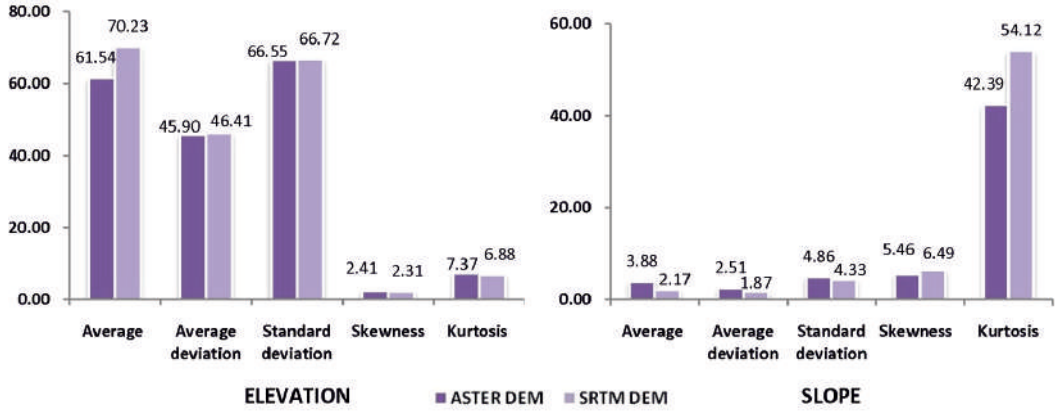

Fig. 14 Comparison of moment statistics of ASTER and SRTM DEMs

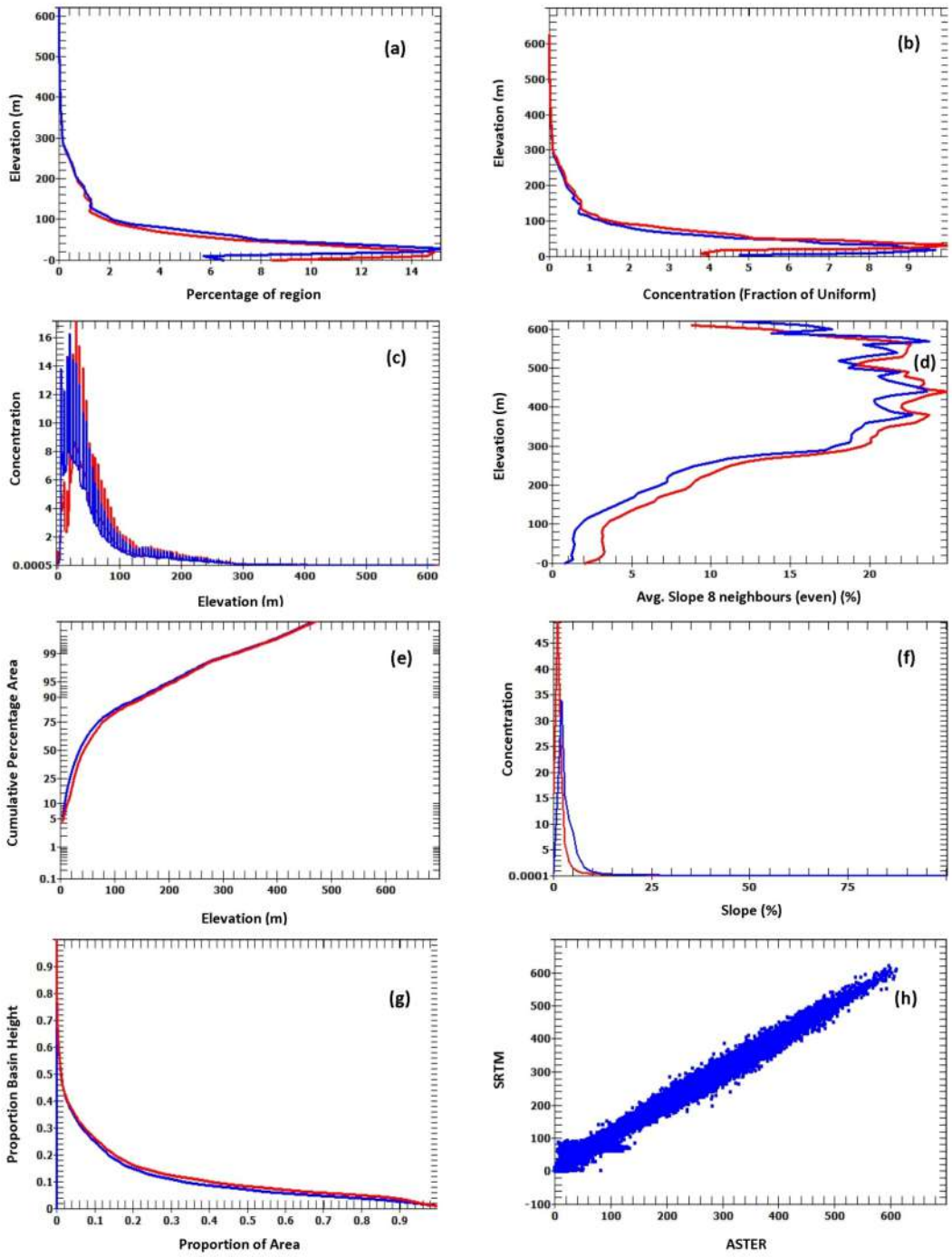

Fig. 15 Comparison of statistical graphs of ASTER and SRTM DEMs: (a) Histogram of elevation, (b) elevation versus concentration (fraction of uniform), (c) concentration versus elevation, (d) elevation versus average slope 8 neighbours (even) (%), (e) cumulative percentage area versus elevation, (f) concentration versus slope, (g) cumulative Strahler curve, (h) Scatter plot of ASTER and SRTM DEMs

For the present study, eight nearest neighbours with even weighting aspect algorithm (Guth, 1995) was used. Aspects of the study area for both DEMs (Fig. 16) by slope categories indicated that the distribution of aspects clearly varies with slope. In the lower slopes, spikes in the aspect distribution were prominent. Aspect algorithms did not work well in low relief regions, producing too many aspects at 45° intervals. Aspects at 45° intervals were over represented, and the algorithm appeared to work well and almost uniformly distributed only when the slope exceeded 30 and 20% for ASTER and SRTM DEMs, respectively. The algorithm produced too many aspects in the 8 principal compass directions, which indicated its performance problem in gentle sloping regions. Each aspect rose (Fig. 16) has a computed Queen's Aspect ratio, which is the ratio of the number of aspects in each of the principal directions compared to the number that would occur if all 360 directions occurred with equal likelihood. A Queen's aspect ratio of 1 indicates no bias in the DEM and algorithm. Queen's aspect ratio for slopes greater than 30% for ASTER and 20% for SRTM is around 1, but its value increases with decrease in slope. Eight neighbour evenly-weighted slope algorithms were used to produce natural slope distributions as it outperforms other algorithms on comparison. With elevation resolution of 90 m, the basic slope values only change by 1/90. Aspect distributions (Fig. 16) for a 30 m DEM with slope values to change by 1/30, and the algorithm appears to produce uniform and natural aspect distributions if the slope is steeper than 30%.

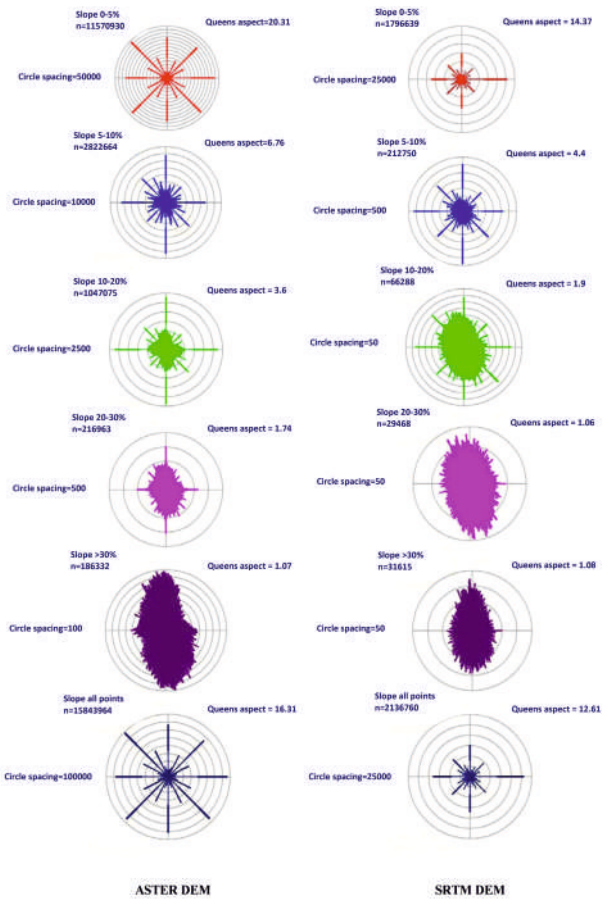

Fig. 16 Aspect distribution by slope for ASTER and SRTM DEMs

The correlation coefficients for both DEMs exceeded 0.99. Average slope and average elevation also exceed 0.99, but such correlation coefficients still allow some scatter and some significant anomalies. In an area that is relatively flat, a difference of two meters in

elevation could mean the loss or saving of thousands of hectares of important agricultural area. Different scale of DEMs accurately captures average elevation, average slope and terrain organization, both in orientation and magnitude, which correlates very strongly across scales. The correlation is weakest in low slope regions, probably because of problems with the aspect algorithms, and strongest in moderate to high relief areas.

4.8 Drainage Network Extraction using ASTER and SRTM DEMs

For ASTER DEM, two threshold values (147.07 and 73.54 km^2) were used for drainage network delineation. Initially in ArcHydro, threshold value of 147.07 km^2 (default area) was used for delineation process and same threshold value was also used in ArcSWAT. Secondly, minimum area (73.54 km^2) provided by ArcSWAT was used for delineation. Similarly, it was done for SRTM DEM with two threshold values (203.37 and 101.69 km^2). Results indicated that delineated drainage network is affected by different DEM and tools used. The reliability of extracted drainage networks depends on the geomorphological characteristic of the terrain. During drainage networks extraction, the focus was on positional accuracy, comparing the central lines of the extracted river networks from both the DEM data. Visual assessment shows that both DEM-derived networks provide relatively accurate depictions of the main streams, but not too accurate for the lower order streams. Drainage network from SRTM DEM are well represented and without any significant errors. In general, SRTM DEM showed less overall errors than the ASTER DEM (Figs. 17 and 18). SRTM DEM produced good results, and mostly matched with reference drainage. SRTM vectors, on the whole, seem to be linearized and lack of some small drainages. However, in many areas the ASTER DEM generated excessive artifacts. Despite the fact that SRTM has greater pixel size, comparison with ASTER indicated that the drainage network obtained from SRTM was the closest to the reference drainage network. Drainage extraction based on ASTER

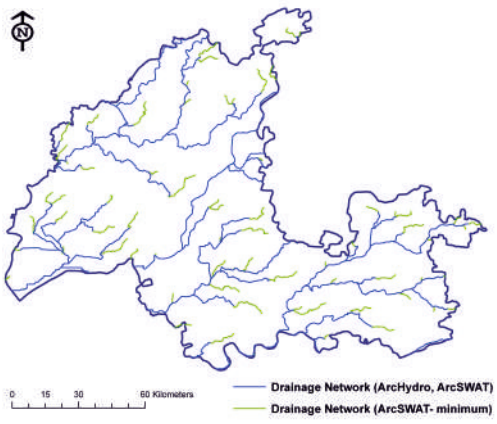

Fig. 17 Drainage networks obtained from ASTER DEM

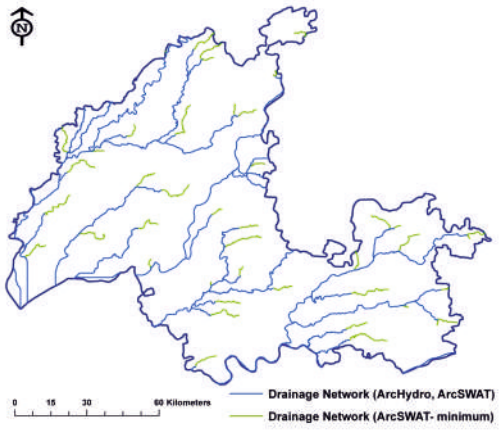

Fig. 18 Drainage networks obtained from SRTM DEM

DEM processing seems to be susceptible to smooth topographic variations and sink areas, and in this way produces commission errors (generate many inexistent drainage vectors). This difference is clearly visible from the Figs. 17 and 18. Visual inspection of the extracted networks indicated following observations. Although ASTER DEM in general produced more streams than SRTM, the extracted networks from SRTM was reasonably accurate than ASTER and also in depicting higher order streams. When both the extracted network was compared with manually delineated reference network, SRTM derived network was more accurate than ASTER despite of its lower resolution. There was some difference in their overall network density levels. Another important and interesting observation is that lower resolution data may not lose more information than higher resolution data. In general, the analysis confirmed the conclusions of previous studies that the SRTM DEM shows less total errors and gave more accurate representation of the main drainage channels than the ASTER DEM. Despite of the higher resolution, the ASTER DEM contains more vertical errors than the SRTM DEM.

Extracted drainage networks from both the DEMs showed deviations (Fig. 19) from reference network. All the points (9250) on SRTM network deviated up to maximum of 5000 m, where as ASTER network deviated up to 50000 m. Deviation of 97.19% points was below 3000 m for SRTM network as compared to 76.48% for ASTER. Up to 40000 m, 93.33% points were covered in ASTER. Drainage network from ASTER showed more deviation as compared to SRTM DEM.

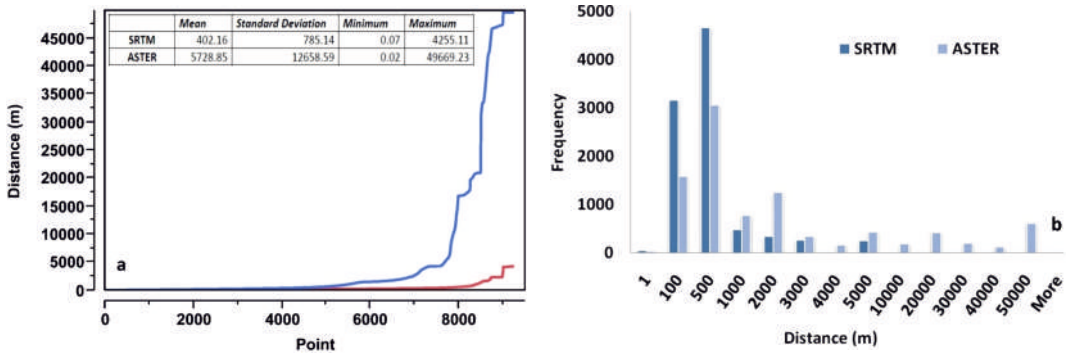

Fig. 19 Distribution of points with (a) Frequency and (b) Distance

4.9 Evaluation of Depressions and the Drainage Area

Mahi is the major river that flows across the study area. Major depressions in the study area are around flood plain (Fig. 20) of Mahi River in its lower sub basin and Khambhat. It is also called Cambay, a port town in Kheda district, which lies at the head of the Gulf of Khambhat and the mouth of the Mahi River. Areas around Khambhat have low bottom elevation (2, 1, and 2 m) and fill depth (3, 4, and 3 m) with depression drainage areas of 36, 33.5, and 21 km^2, respectively. These areas are more susceptible to flood.

Due to its lower elevation and fill depth of 9 m with depression drainage area of around 68 km^2, flood plain of lower Mahi river sub basin is more prone to flood and damage. Water bodies extracted for pre- and post-flooding periods also support the present analysis. Depressions mapping helped in identifying spatial flood susceptible areas and its geometric features.

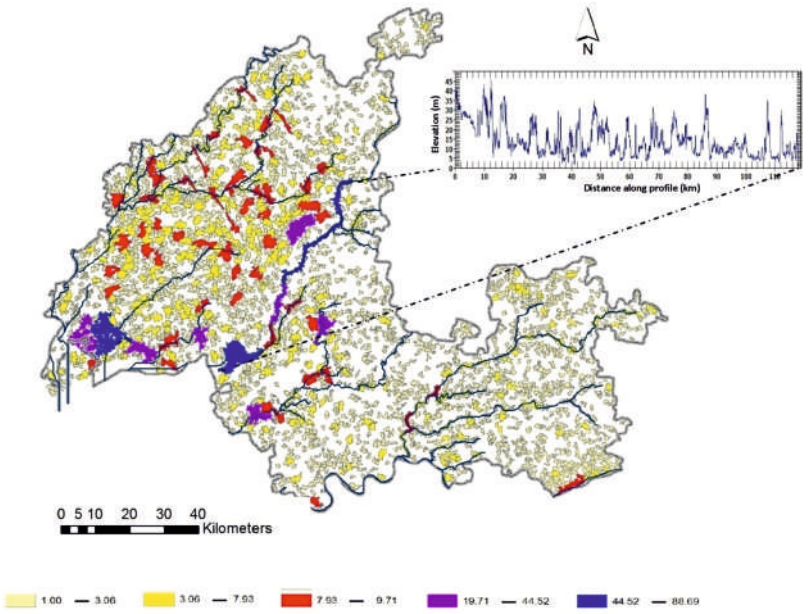

Fig. 20 Spatial mapping of depressions with drainage area (km^2)

4.10 Change Detection in Drainage Network for Pre- and Post-Flooding Periods

Major changes in the drainage network as a result of flood were observed. Out of 10000 points, 5.22% showed deviation between 100-300 m (October, 2004-05), indicating the effect of flood (Fig. 21). No change in drainage network was observed (deviation < 1m) at 61.45% points. During February (2005-06), deviation (100-300 m) was observed in drainage network at 3.18% points and no change at 82.23% points. Changes in the drainage network due to flood at different location in the study area and deviation (> 100 m) with angular direction for the period October 2004-05 are shown in Figs. 22 and 23, respectively. Similarly, Changes in the drainage network due to flood at different location in the study area and deviation (> 100 m) with angular direction for the period February 2005-06 are depicted in Figs. 24 and 25, respectively. These changes suggest that the drainage pattern is highly dynamic and subject to instability in response to major flood events. Overall, the study results showed that the drainage

network extraction with magnitude and directional change analysis, which is one of the essential factors on flood disaster assessment, is viable and effective, and can assist in post-flood disaster assessment. It is necessary to take major management steps to recover the stability of the system. In future, similar evaluations with consideration of more geomorphological and topographic characteristics in different study areas need to be taken up to verify the robustness of the results obtained.

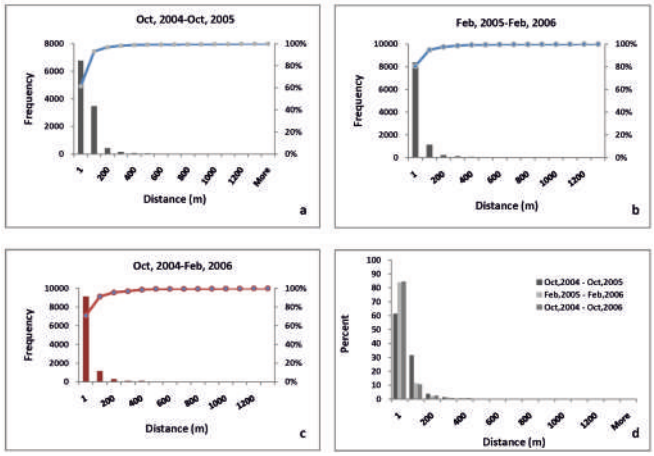

Fig. 21 Frequency distribution of changed position (a) Oct, 2004-Oct, 2005; (b) Feb, 2005-Feb, 2006; (c) Oct, 2004-Feb, 2006 along with (d) Percentage of points deviated by distance

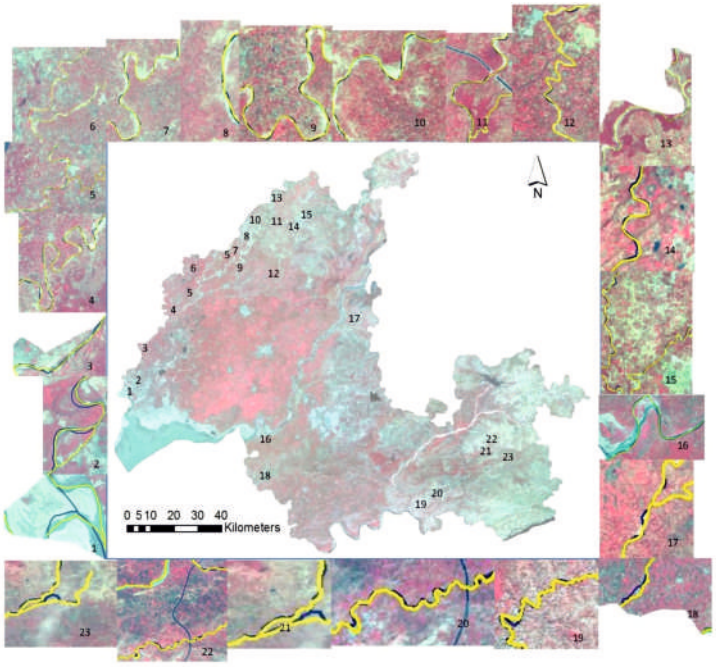

Fig. 22 Drainage network change for October, 2004-2005

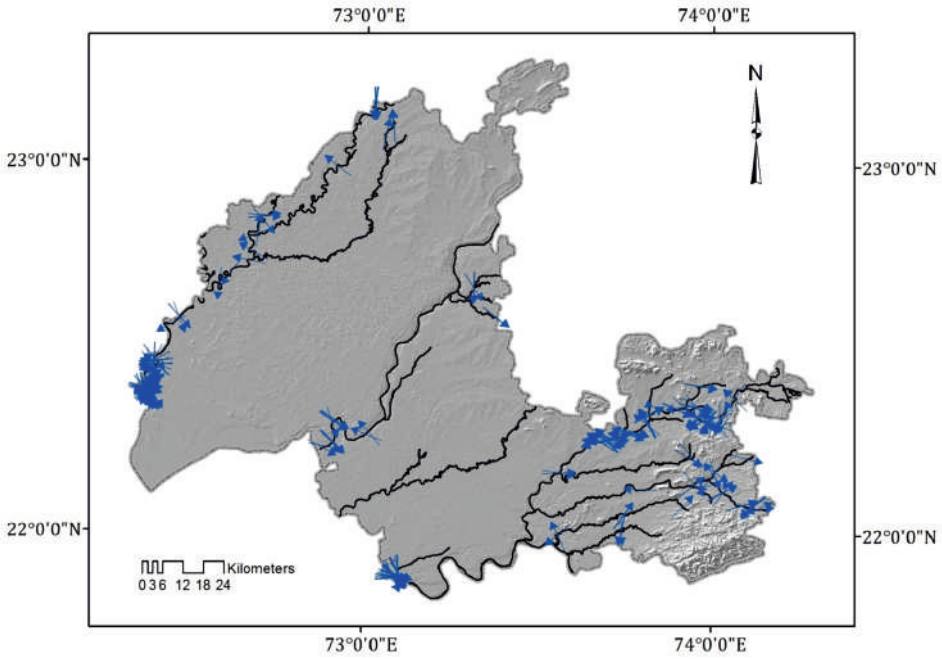

Fig. 23 Location for change greater than 100 m with angular direction (October, 2004–2005)

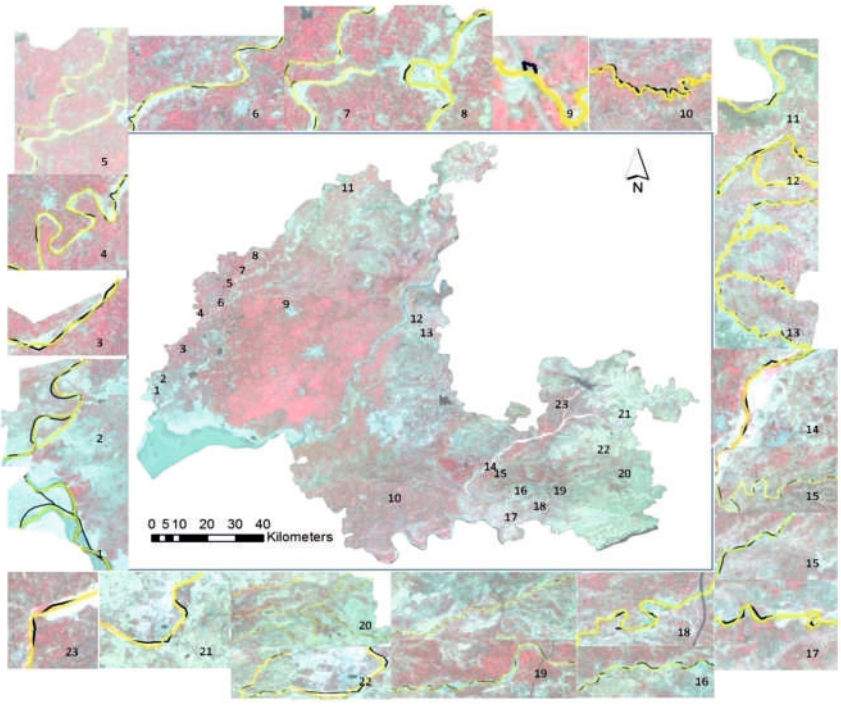

Fig. 24 Drainage network change for February, 2005-2006

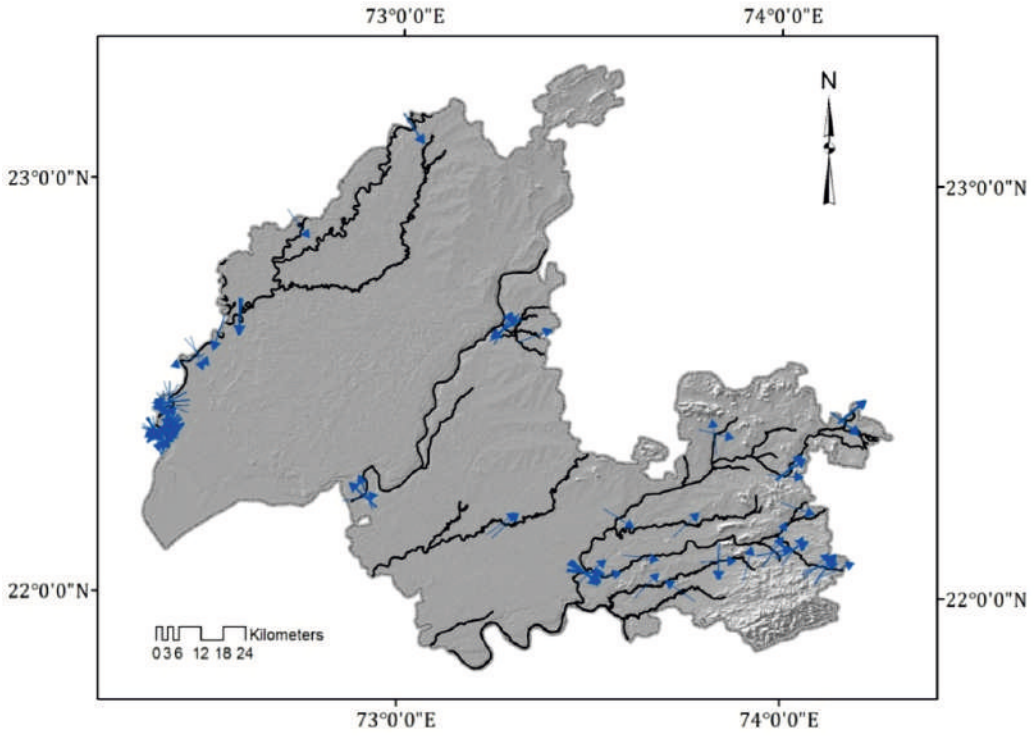

Fig. 25 Location for change greater than 100 m with angular direction (February, 2005–2006)

5. SUMMARY AND CONCLUSIONS

The study has demonstrated the use of remote sensing and GIS in systematic analysis of LULC and water bodies mapping, change detection, geomorphology, and drainage network in the event of flood. It has also helped in understanding the spatial and temporal distribution of LULC, water bodies and drainage network along with changes caused due to flood. The LULC and water bodies were mapped for two seasons for pre- as well as post-flooding periods. The geomorphology, drainage morphometry, depressions, and changes in drainage network due to flood were analyzed. The importance of DEM in geomorphometry, drainage network, and depressions generation based study was emphasized. The impact of different sources of DEM data on the outcome of hydrologic applications, mainly river network extraction, was evaluated.

The LULC of the study area is diverse and complex, comprising both homogeneous and heterogeneous surface features, causing problems of spectral variability in the satellite image data. In order to improve mapping accuracies from remotely sensed data, relying on only one approach was not enough. Thus, three approaches (unsupervised, supervised, fuzzy based) were used to extract LULC information. Results revealed that some classes could be separated even better by using soft computing technique such as fuzzy logic. The fuzzy approach presented more accurate results in terms of separating the classes as compared to traditional pixel-based classification approach (supervised and unsupervised) for improving the LULC information. Further, the accuracy assessment showed that the fuzzy approach could predict LULC more accurately. It has great potential in mapping of flood induced LULC with low difference in the errors of omission and commission.

Unsupervised classification results for the period October 2004 to October 2005 revealed decrease in inland water bodies (14.49%) and agricultural area (6.42%) and increase in remaining LULC. In February 2005 to February 2006, all LULC classes decreased except agricultural fallow and sparse vegetation. In case of supervised classification, from October 2004 to October 2005, decrease was observed only in agricultural area (6.78%). Similarly, in February 2005 to February 2006, increase in coastal water bodies (0.73%) and sparse vegetation (1.7%) was observed and in remaining LULC classes decrease was noticed. In fuzzy based classification, only decrease in agricultural area (7.09%) was observed from October 2004 to October 2005, whereas during February 2005 to February 2006, decrease in area was exhibited in all LULC classes except coastal water bodies and sparse vegetation. The effect of flood was more prominently observed in monsoon season as compared to winter or dry season. Among all the LULC classes, agriculture was most affected due to flood. Agriculture was classified more accurately in all the classification approaches with

small variation. Careful judgment of spectrally similar classes is essential before merging and labeling of clusters in unsupervised classification as results indicated some misclassification.

Spatial distribution of water bodies were extracted using radiance image of IRS P6 LISS III and standard water indices. Results confirmed the better accuracy of MNDWI in separating water bodies. Area under water bodies increased by 10.4% between October 2004-2005 and 3.8% between February 2005-2006, which was primarily due to flood. Thus, MNDWI was found to be more efficient and reliable in detecting water bodies, whereas NDWI over estimated the same. Mapping of water bodies provided useful information on spatial water distribution and thereby effect of flood in the study area. Present methodology can be helpful in similar study where the assessment of water resources and flood inundation is of prime importance.

The application of DEM data provided significant information on geomorphology, characterizing drainage networks, and flood susceptible or vulnerable area. Results indicated some difference in elevation information representing uncertainty in DEM. The study area is relatively flat in topography. The extreme values of elevation and slope affected the moment statistic of both the DEMs. The distribution of aspects in the study area clearly varied with slope. In the lower slopes, spikes in the aspect distribution were prominent and the algorithm did not work well in low relief regions. Morphometric analysis based on extracted drainage networks from SRTM has shown better results than ASTER DEM. The SRTM data, although of coarser spatial resolution, represented the actual topography more accurately than the ASTER DEM. It performed reasonably well on moderately sloped or flat topography, which is the characteristic of our study area. Despite of its higher resolution, ASTER DEMs did not indicate any advantage in deriving drainage networks of lower order. The reliability of extracted drainage networks is dependent on the geomorphological characteristic of the terrain. GIS-based approach in studying the geomorphological characteristics was observed more appropriate over conventional methods. The present methodology also identified the depressions for the flood vulnerable areas. It can help to delineate flood prone areas to bring down probable damages in flood susceptible pockets which suffer from inadequate hydrological information. Change analysis of drainage pattern indicated that 5.22% (October, 2004-05) and 3.18% (February, 2005-06) points deviated between 100-300 m.

The observed water bodies and drainage network of different time periods associated to extreme flood events showed significant changes. Study on dynamic aspects of drainage network caused due to flood detected important movement in magnitude as well as direction. These changes suggest that the drainage pattern is highly dynamic and subject to instability in response to major flood events. The study result showed that the drainage network extraction with magnitude and directional change analysis,

which is one of the essential factors on flood disaster assessment, is viable and effective, and can assist in post-flood disaster assessment. In order to restore and recover the stability of the system, it is recommended to perform post-flood management measures. In overall, integrated use of remote sensing and GIS can be effectively used to understand the geomorphology along with spatial and temporal dynamics of water bodies and drainage network. The water bodies and drainage network changes detected and interpreted in the present work can help and support future studies to reveal the pattern and reasons for spatio-temporal changes due to flood. The study helps in understanding the various levels of protections needed to minimize and prevent damage due to devastating flood. The approach followed in this study, hopefully will help in carrying out further studies on water resources planning and flood management.

6. REFERENCES

1. Anderson JR, Hardy EE, Roach JT, Witmer RE (1976) A land use and land cover classification system for use with remote sensor data. US Geological Survey Professional Paper No. 964. Washington, DC
2. Bhagwat TN, Shetty A, Hegde VS (2011) Spatial variation in drainage characteristics and geomorphic instantaneous unit hydrograph (GIUH); implications for watershed management - A case study of the Varada River basin, Northern Karnataka. Catena 87(1):52–59
3. Bishop MP, Shroder JF (2004) Geographic Information Science and Mountain Geomorphology. Heidelberg: Springer Praxis Books, pp 486
4. Congalton RG (1991) A review of assessing the accuracy of classifications of remotely sensed data. Remote Sensing of Environment 37: 35–46
5. Congalton RG, Green K (1999) Assessing the Accuracy of Remotely Sensed Data: Principles and Practices, Boca Raton: Lewis, pp 137
6. Coppin P, Jonckheere I, Nackaerts K, Muys B, Lambin E (2004) Digital change detection methods in ecosystem monitoring: A review. International Journal of Remote Sensing 25: 1565–1596
7. Dewan AM, Nishigaki M, Kumamoto T (2007) Evaluating flood hazard for land-use planning in Greater Dhaka of Bangladesh using remote sensing and GIS techniques. Water Resources Management 21(9): 2101–2116
8. Fan F, Weng Q, Wang Y (2007) Land use / land cover change in Guangzhou, China, from 1998 to 2003, based on Landsat TM/ETM+ imagery. Sensors 7(7): 1323-1342
9. Foody GM, Atkinson PM (2002) Uncertainty in remote sensing and GIS. John Wiley & Sons, Chichester, UK
10. Foody GM (2002) Status of land cover classification accuracy assessment. Remote Sensing of Environment 80(1): 185-201
11. Frankel KL, Dolan JF (2007) Characterizing arid region alluvial fan surface roughness with airborne laser swath mapping digital topographic data. Journal of Geophysical Research: Earth Surface 112: F02025, doi:10.1029/ 2006JF000644
12. Guth PL (1995) Slope and aspect calculations on gridded digital elevation models: Examples from a geomorphometric toolbox for personal computers. Zeitschrift für Geomorphologie N.F., Supplement band 101:31–52
13. Henshaw AJ, Gurnell AM, Bertoldi W, Drake NA (2013) An assessment of the degree to which Landsat TM data can support the assessment of fluvial dynamics, as revealed by changes in vegetation extent and channel position, along a large river. Geomorphology 202: 74-85
14. Jain SK, Singh RD, Jain MK, Lohani AK (2005) Delineation of Flood-Prone Areas Using Remote Sensing Techniques. Water Resources Management (2005) 19: 333–347
15. Jain SK, Saraf AK, Goswami A, Ahmad T (2006) Flood inundation mapping using NOAA AVHRR data. Water Resources Management 20:949–959

16. James LA, Watson DG, Hansen WF (2007) Using LiDAR data to map gullies and headwater streams under forest canopy: South Carolina, USA. Catena 71:132–144

17. Jensen JR (2005) An introductory digital image processing: A remote sensing perspective. Prentice Hall, New Jersey, pp 526

18. Jones AF, Brewer PA, Johnstone E, Macklin MG (2007) High-resolution interpretative geomorphological mapping of river valley environments using airborne LiDAR data. Earth Surface Processes and Landforms 32:1574–1592

19. Ji L, Zhang L, Wylie B (2009) Analysis of dynamic thresholds for the Normalized Difference Water Index. Photogrammetric Engineering and Remote Sensing 75:1307–1317

20. Kundzewicz ZW, Hirabayashi Y, Kanae S (2010) River Floods in the Changing Climate—Observations and Projections. Water Resources Management 24: 2633-2646

21. Leica Geosystems (2008) ERDAS Field Guide, Volume Two. Norcross, Georgia Leica Geosystems Geospatial Imaging, LLC, pp 384

22. Lillesand TM, Kiefer RW, Chipman JW (2008) Remote sensing and image interpretation. New York: John Wiley & Sons, Inc

23. Machado SM, Ahmad S (2007) Flood hazard assessment of Atrato River in Colombia. Water Resources Management (2007) 21:591–609

24. Mark DM (1984) Automatic detection of drainage networks from digital elevation models. Cartographica 21:168–178

25. Martz LW, Garbrecht J (2007) Automated extraction of drainage network and watershed data from digital elevation models. Journal of the American Water Resources Association 29:901–908

26. Mas J (1999) Monitoring land-cover changes: a comparison of change detection techniques. International Journal of Remote Sensing 20(1): 139-152

27. Mason DC, Scott TR, Wang HJ (2006) Extraction of tidal channel networks from airborne scanning laser altimetry. ISPRS Journal of Photogrammetry and Remote Sensing 61:67–83

28. McFeeters SK (1996) The use of the Normalized Difference Water Index (NDWI) in the delineation of open water features. International Journal of Remote Sensing 17:1425–1432

29. Ministry of Water Resources (2002) National water policy. Ministry of Water Resources, Government of India, New Delhi, pp 10

30. Notebaert B, Verstraeten G, Govers G, Poesen J (2009) Qualitative and quantitative applications of LiDAR imagery in fluvial geomorphology. Earth Surface Processes and Landforms 34:217–231

31. Ozdemir H, Bird D (2009) Evaluation of morphometric parameters of drainage networks derived from topographic maps and DEM in point of floods. Environmental Geology 56:1405–1415

32. Patel, DP, Srivastava PK (2013) Flood Hazards Mitigation Analysis Using Remote Sensing

and GIS: Correspondence with Town Planning Scheme. Water Resources Management 27:2353–2368

33. Reddy GPO, Maji A, Gajbhiye KS (2004) Drainage morphometry and its influence on landform characteristics in basaltic terrain, central India—a remote sensing and GIS approach. International Journal of Applied Earth Observation and Geoinformation 6:1–16

34. Robinove CJ (1982) Computation with physical values from Landsat digital data. Photogrammetric Engineering and Remote Sensing 48(5):781–784

35. Serra P, Pons X, Saurı´ D (2008) Land-cover and land-use change in a Mediterranean landscape: a spatial analysis of driving forces integrating biophysical and human factors. Applied Geography 28:189–209

36. Sharma CS, Behera MD, Mishra A, Panda SN (2011) Assessing flood induced landcover changes using remote sensing and fuzzy approach in eastern Gujarat (India). Water Resources Management 25(13):3219-3246

37. Shalaby A, Tateishy R (2007) Remote sensing and GIS for mapping and monitoring land cover and land use changes in the Northwestern coastal zone of Egypt. Applied Geography 27: 28–41

38. Singh A, (1989) Digital change detection techniques using remotely sensed data. International Journal of Remote Sensing 10 (6): 989–1003

39. Strahler AN (1952) Hypsometric (area-altitude) analysis of erosional topography. Geological Society of America Bulletin 63:1117–1141

40. Tucker CJ (1979) Red and photographic infrared linear combinations for monitoring vegetation. Remote Sensing of Environment 8: 127–150

41. Thomas J, Joseph S, Thrivikramji K, Abe G, Kannan N (2012) Morphometrical analysis of two tropical mountain river basins of contrasting environmental settings, the southern Western Ghats. India. Environmental Earth Sciences 66(8):2353–2366

42. Tribe A (1992) Automated recognition of valley lines and drainage networks from grid digital evolution models: a review and a new method. Journal of Hydrology 139:263–293

43. Wang F (1990) Fuzzy supervised classification of remote sensing images. IEEE Transactions on Geoscience and Remote Sensing 28(2): 194-201

44. Yuan F, Sawaya KE, Loeffelholz B, Bauer ME (2005) Land cover classification and change analysis of the twin cities (Minnesota) metropolitan areas by multitemporal Landsat remote sensing. Remote Sensing of Environment 98(2): 317-328

45. Xu H (2006) Modification of normalised difference water index (NDWI) to enhance open water features in remotely sensed imagery. International Journal of Remote Sensing 27:3025–3033

46. Zadeh L A (1965) Fuzzy sets. Information and Control 8(3): 338 – 353